11F

NUREG/CR-3350
PNL-4933

LOCA Simulation in the National Research Universal Reactor Program

Postirradiation Examination Results for the Third Materials Experiment (MT-3)

Prepared by W. N. Rausch

Pacific Northwest Laboratory
Operated by
Battelle Memorial Institute

Prepared for
U.S. Nuclear Regulatory Commission

GPO Printed copy price: $4.50

NUREG/CR-3350
PNL-4933
R3

LOCA Simulation in the National Research Universal Reactor Program

Postirradiation Examination Results for the Third Materials Experiment (MT-3)

Manuscript Completed: February 1984
Date Published: April 1984

Prepared by
W. N. Rausch

Pacific Northwest Laboratory
Richland, WA 99352

Prepared for
Division of Accident Evaluation
Office of Nuclear Regulatory Research
U.S. Nuclear Regulatory Commission
Washington, D.C. 20555
NRC FIN B2277

ACKNOWLEDGMENTS

The author would like to thank R. R. Lewis for overseeing the postirradiation examination of the MT-3 fuel rods, and for his assistance in organizing the collected data.

ABSTRACT

A series of in-reactor experiments were conducted by Pacific Northwest Laboratory using full-length 32-rod pressurized water reactor (PWR) fuel bundles as part of the Loss-of-Coolant Accident (LOCA) Simulation Program. The third materials experiment (MT-3) was the sixth in the series of thermal-hydraulic and materials deformation/rupture experiments conducted in the National Research Universal (NRU) reactor, Chalk River, Ontario, Canada. The MT-3 experiment was jointly funded by the U.S. Nuclear Regulatory Commission (NRC) and the United Kingdom Atomic Energy Authority (UKAEA). The main objective of the experiment was to evaluate ballooning and rupture during active two-phase cooling in the temperature range from 1400 to 1500°F (1030 to 1090K). The 12 test rods in the center of the 32-rod bundle were initially pressurized to 550 psi (3.8 MPa) to insure rupture in the correct temperature range. All 12 of the rods ruptured, with an average peak bundle strain of ~55%.

The UKAEA also funded destructive postirradiation examination (PIE) of several of the ruptured rods from the MT-3 experiment. This report describes the work performed and presents the PIE results. Information obtained during the PIE included cladding thickness measurements, metallography, and particle size analysis of the cracked and broken fuel pellets.

SUMMARY

The Loss-of-Coolant Accident (LOCA) Simulation Program was conducted by Pacific Northwest Laboratory to evaluate the thermal-hydraulic and mechanical deformation behavior of full-length light-water reactor (LWR) fuel bundles under LOCA conditions. The tests were designed to simulate the heatup, reflood, and quench phases of a large-break LOCA; and were performed in the National Research Universal (NRU) reactor using nuclear fission to simulate the low-level decay power typical of these conditions.

The sixth experiment in the program--Materials Test 3 (MT-3)--was jointly funded by the U.S. Nuclear Regulatory Commission (NRC) and the United Kingdom Atomic Energy Authority (UKAEA). The main objective of the MT-3 experiment was to obtain data pertinent to the licensing requirements for ballooning and blockage of fuel rod cladding. By agreement with the NRC, the test conditions were identified and selected by the UKAEA.

This document presents the postirradiation examination (PIE) results for several of the ruptured rods from the MT-3 experiment. Particle size analyses of the fuel from various rod sections were conducted, and metallographic specimens of the Zircaloy cladding from these sections were prepared and examined. Rod sections were chosen to include the most severely deformed and ruptured locations in the test rods.

Metallographic examination of the Zircaloy cladding revealed that temperatures were not sufficient to cause any alpha-beta transformation, but that some grain growth had occurred. Evidence of cold work (twinning) was prevalent in areas where the cladding was deformed.

Oxidation occurred on both the inner and outer surfaces of the cladding. The oxide thickness on the inside surface never averaged more than 2 μm and was usually between 0.5 μm and 1 μm. The average oxide thickness on the outer surface of the cladding was greater (~4 μm), especially at the elevations where the axial temperature profile peaked, i.e., around the failure sites.

Circumferential cladding thickness measurements were made to determine whether there was a "spiraling" of cladding wall thickness. Lengths of cladding varying from 12 to 18 in. (300 to 450 mm) were sectioned at 1.00-in. (25.4 mm) intervals. No spiraling trend was evident.

The size analysis of the fuel particles revealed that two pellets from one of the rod sections were still intact. The rest of the pellets cracked into particles, 96% of which were 0.111 in. (2.8 mm) and larger.

CONTENTS

FIGURES

TABLES

INTRODUCTION

A series of in-reactor experiments were conducted by Pacific Northwest Laboratory (PNL)[a] using full-length 32-rod pressurized water reactor (PWR) fuel bundles as part of the Loss-of-Coolant Accident (LOCA) Simulation Program (Hann 1979). The third materials experiment (MT-3) was the sixth in the series of thermal-hydraulic and materials deformation/rupture experiments conducted in the National Research Universal (NRU) reactor at Chalk River Nuclear Laboratory (CRNL),[b] Chalk River, Ontario, Canada. The experiment was jointly funded by the U.S. Nuclear Regulatory Commission (NRC) and the United Kingdom Atomic Energy Authority (UKAEA).

The main objective of MT-3 was to evaluate the ballooning and rupture behavior of the cladding during active two-phase cooling in the temperature range from 1400 to 1500°F (1030 to 1090K). The 12 test rods in the center of the 32-rod bundle were initially pressurized to 550 psi (3.8 MPa) to simulate a PWR rod at beginning-of-life (Table 1). The MT-3 experiment consisted of a preconditioning phase, a pretransient test phase, and a single transient test (peak cladding temperature ~1050K) (Table 2) in which all 12 test rods ballooned and ruptured. A plot of the peak cladding temperature versus time during the transient test is shown in Figure 1.

After the experiment, the test rods were examined and measured under water using the disassembly, examination, and reassembly machine (DERM) (Mohr et al.

TABLE 1. MT-3 Test Fuel Rod Parameters

Cladding material	Zircaloy-4
Cladding outside diameter (OD)	0.379 in. (0.963 cm)
Cladding inside diameter (ID)	0.331 in. (0.841 cm)
Pitch (rod to rod)	0.502 in. (1.275 cm)
Fuel pellet (OD)	0.325 in. (0.825 cm)
Fuel pellet length	0.375 in. (0.953 cm)
Active fueled length	144 in. (365.75 cm)
Total shroud length	1709.125 in. (423.1 cm)
Helium pressurization	550 psig (3.8 MPa)
Fuel enrichment	2.93% ^{235}U

(a) Operated for the U.S. Department of Energy (DOE) by Battelle Memorial Institute.
(b) Operated by Atomic Energy of Canada, Ltd. (AECL).

TABLE 2. Measured Experiment Operation Conditions

	Reactor Power, MW	Coolant	Steady-State Cladding Temperature, °F	Start Time	Delta Time (min:sec)
Preconditioning	127	Water	-	11/12/81 06:30	04:35
Reflood calibration	0	Steam/reflood water	-	11/12/81 19:15	00:15
MT-3.01 adiabatic	6.7	Steam	810	11/12/81 20:47	01:02
MT-3.02 DACS scram abort	0	-	-	-	-
MT-3.03 abort level check	1.8	Steam	500	11/12/81 22:31	00:22
MT-3.04 adiabatic	7.2	Steam	835	11/12/81 23:06	00:26
MT-3.05 flow rate check	1.8	Steam/reflood water	500	11/12/81 23:35	00:19
MT-3.06 transient	7.2	Reflood water	835	11/13/81 00:14	00:32 (00:18 to bundle quench)

1983). Seven rods were then selected for destructive examination in the CRNL hot cells. These rods and their selection criteria are listed in Table 3. A detailed metallographic examination of the cladding was performed around the ruptured region of each rod. Cladding thickness measurements were made from photographs of the fuel rod cross sections. For several of the rods, additional cross sections were measured at distances up to 21 in. (530 mm) from the rupture site. A particle size analysis of the fuel was also performed on a section of each rod.

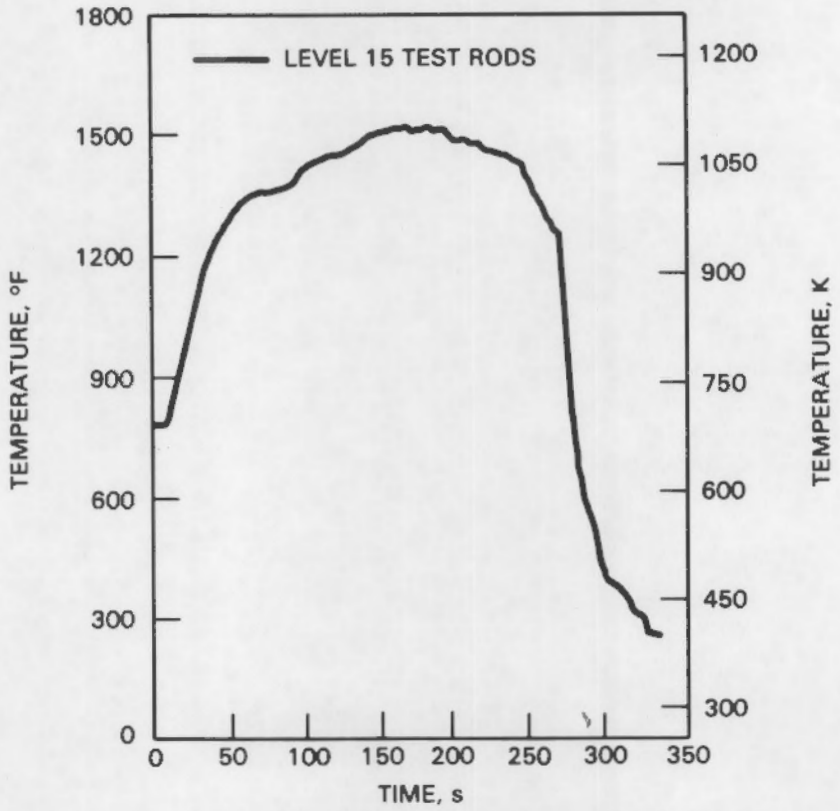

FIGURE 1. MT-3 Peak Cladding Temperature

TABLE 3. MT-3 Rods Selected for Postirradiation Examination

Rod	Criteria
5C	Longest time to rupture
3B	Shortest time to rupture
4B	Smallest rupture strain
5D	Lowest temperature rupture
3E	Highest temperature rupture
3D	"Average strain" rod
2D	Pinhole rupture

DESCRIPTION OF THE POSTIRRADIATION EXAMINATION

After the DERM examination, seven rods (Table 3) were selected for further examination of the cladding and fuel: 2D, 3B, 3D, 3E, 4B, 5C, and 5D. Sections ~18 in. (46 cm) long, including the failure region, were cut from each of these rods. In addition, two 12-in. (30-cm) sections were cut from Rod 3B: one from below the rupture site and one from above. This work was done in the universal cells in mid-October 1982, and the samples were then sent to the hot cells in building 375 at CRNL for detailed PIE.

The locations of the metallographic samples were determined from photographs and from reference scribe marks made during the DERM analysis. A small high-speed cut-off saw with a diamond wheel was used to make cuts 0.08 to 0.12 in. (2 to 3 mm) from the scribe marks. Because the bulged and distorted cladding made the use of a standard vise impossible, a toggle-type clamp and a V-groove were used. The sections were placed in the V-groove and then leveled by eye using small wooden wedges. Once the section appeared level, it was fastened in place with the toggle clamp.

For each cladding sample, the distance from the cut to the pertinent scribe mark was measured to within 0.02 in. (0.5 mm) and recorded (Table 4). The samples were cold-mounted in bio-plastic to eliminate any possibility of deformation. All samples were ground and polished to within 0.02 in. (0.5 mm) of the desired locations by measuring the amount of material removed from the reference face of the sample.

Circumferential cladding thickness measurements were taken of each metallurgical section at regular intervals (chords of 0.050 in. or 1.27 mm) on the microscope viewing screen at 200X magnification. The appearance of the grain structure at different locations along the circumference was also noted, as was the presence of oxygen-enriched layers on the outer and inner surfaces of the cladding.

The destructive examinations performed on the specimens included a circumferential measurement of the cladding wall thickness at different axial positions of the fuel rods, to determine whether there was a spiral pattern to the cladding dimensions.

A particle size analysis was performed on the fuel from the rod sections. Six standard 8-in. (203-mm) diameter sieves were stacked on a portable sieve shaker. The following mesh sizes were used: 0.233 in. (5.60 mm), 0.157 in. (4.00 mm), 0.111 in. (2.80 mm), 0.0787 in. (2.00 mm), 0.0394 in. (1.00 mm), and 0.0117 in. (300 μm). After about 10 min of shaking, each sieve was emptied by brushing the fuel fragments onto a tarred tissue paper, which was then weighed to 0.001 g on a Gram-matic balance in Hot Cell 1.

TABLE 4. Axial Locations of Cladding Cross Sections

MT-3 Rod	Designation[a]	Position[b]
2D	2D5A	105.880
2D	2D5B	105.621
3B	3B5A	105.086
3B	3B5B	103.430
3D	3D5A	105.800
3D	3D5B	105.080
3E	3E5A	106.029
3E	3E5B	105.086
4B	4B5A	101.858
4B	4B5B	105.086
5C	5C5A	106.000
5C	5C5B	105.086
5D	5D5A	106.029
5D	5D5B	105.086

(a) For example, 2D5A = Rod 2D from Assembly 5 (MT-3 was the sixth test in the NRU LOCA program but two of the earlier tests used the same assembly), metallographic section A (two cuts in each rod, one above and one below the rupture).

(b) Elevation (in in.) referenced to the bottom of the fuel in the test bundle.

EXAMINATION RESULTS

Metallographic samples were made from the cross sections of the deformed cladding from each of the rod sections. The mounted and polished samples were photographed, and observations on grain structure appearance were made at different locations along the circumference. The thickness of oxygen-enriched layers on the outer and inner cladding surfaces was also noted. The photographs and observations are presented in Figures 2 through 8. The reproductions of the photos were not of a quality high enough to show the grain structure or oxygen-enriched layers, so features of interest have been marked on the figures.

Oxygen-enriched layers varied in thickness from 0.5 to 2 μm on the inner and outer surfaces of all cladding sections except 5D5B (Figure 9). A summary of the thickness of the oxygen-enriched layers that formed on the specimens is presented in Table 5. Only two sections revealed cracks in the oxygen-enriched layer; these were the two sections from 2D5 that had cracks in the layers both on the outer and inner surfaces in the vicinity of the grossly distorted regions (Figure 10).

The cladding apparently did not reach temperatures high enough to transform the cladding structure from alpha to beta phase, although some growth of the alpha grains was observed (Figure 11). This growth was observed on 2D5A and B, 3B5B, 3D5A and B, 3E5A and B, and 4B5A in certain areas (Figures 2 through 6). Portions of the cladding from 2D5A and B, 3B5B, 3D5A, 3E5A, 4B5A, 5D5A and B, and almost the entire cladding circumference of 5C5A and B displayed evidence of textural banding (clustering of grains that are close to the same orientation); see Figure 12. Figure 13 is typical of the structure, exhibiting small alpha-annealed grains, remote from the cladding ruptures and necked-down areas.

These same grain size and shape phenomena were found in out-of-reactor tests of fuel rods using slow heatup rates. Guenther (1983) found that "there was a direct correlation between heating rate and increased grain size; however, the most significant grain growth occurred at the failure regions where cladding strains were the greatest."

The MT-3 rods showed evidence of cold work (twinning) in areas where the cladding was deformed (Figure 14). Grains and twins were distorted in several areas on the outer surface of the cladding from 3B5A (see Figure 3a for locations). The worst case of this distortion is shown in Figure 15.

Cladding thickness measurements were taken of each metallographic section at regular intervals (chords of 0.050 in. or 1.27 mm) on the microscope viewing screen at 200X magnification. These measurements are listed in Tables 6 through 12.

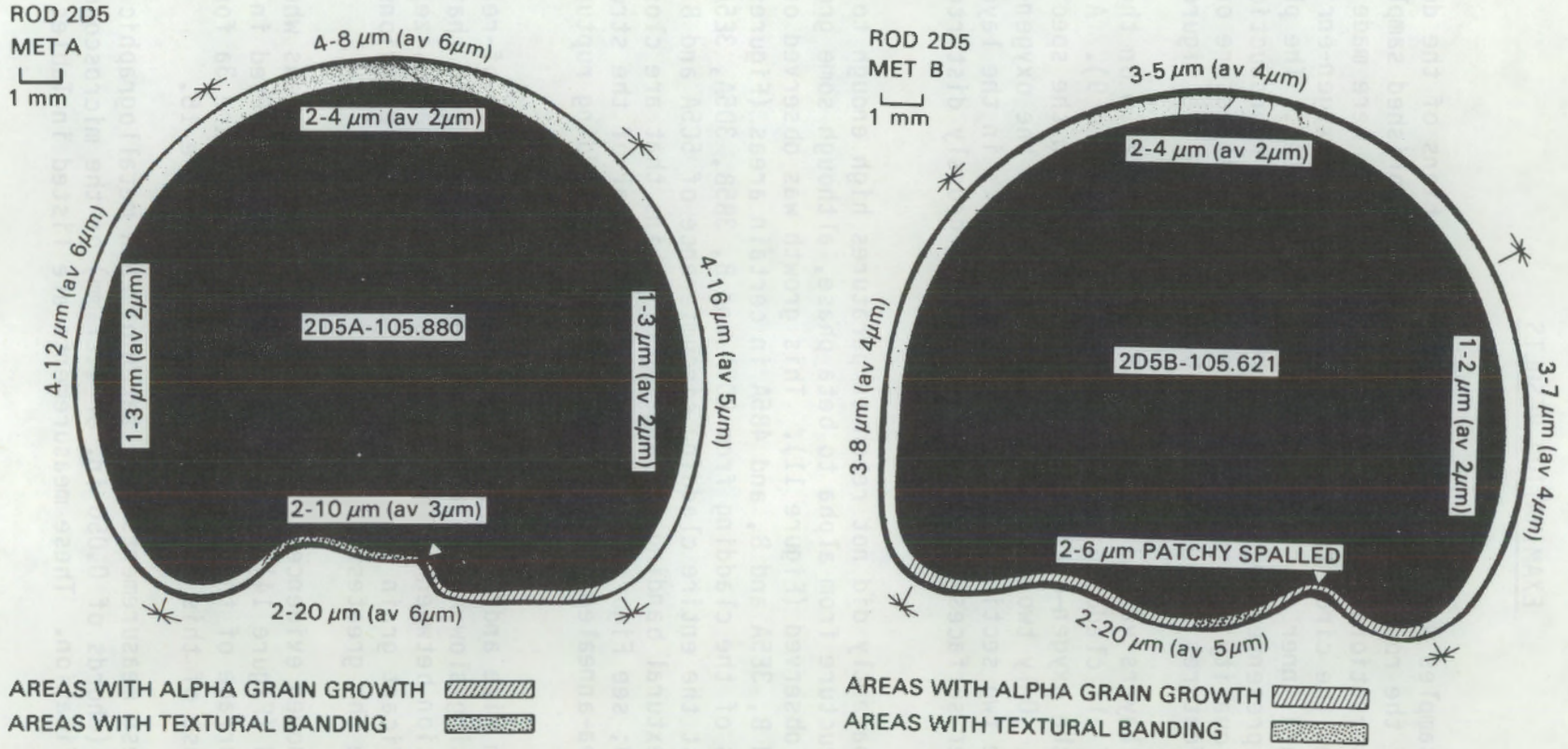

FIGURE 2. Rod Section 2D5, ZrO_2 Thicknesses on Inner and Outer Cladding Surfaces, and Areas with Alpha Grain Growth and Textural Banding. (White triangles indicate the reference point for wall thickness measurements.)

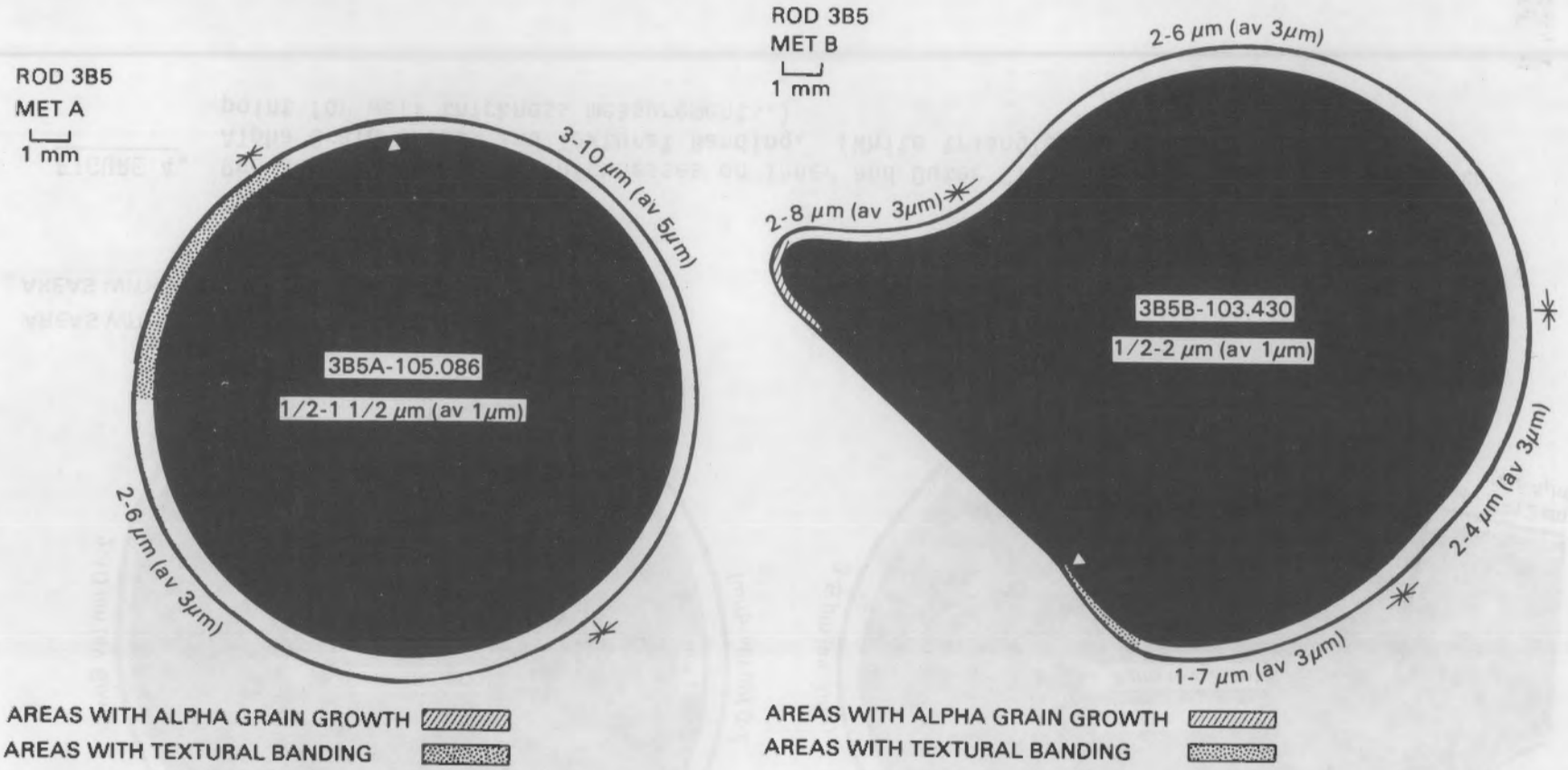

FIGURE 3. Rod Section 3B5, ZrO_2 Thicknesses on Inner and Outer Cladding Surfaces, and Areas with Alpha Grain Growth and Textural Banding. (White triangles indicate the reference point for wall thickness measurements.)

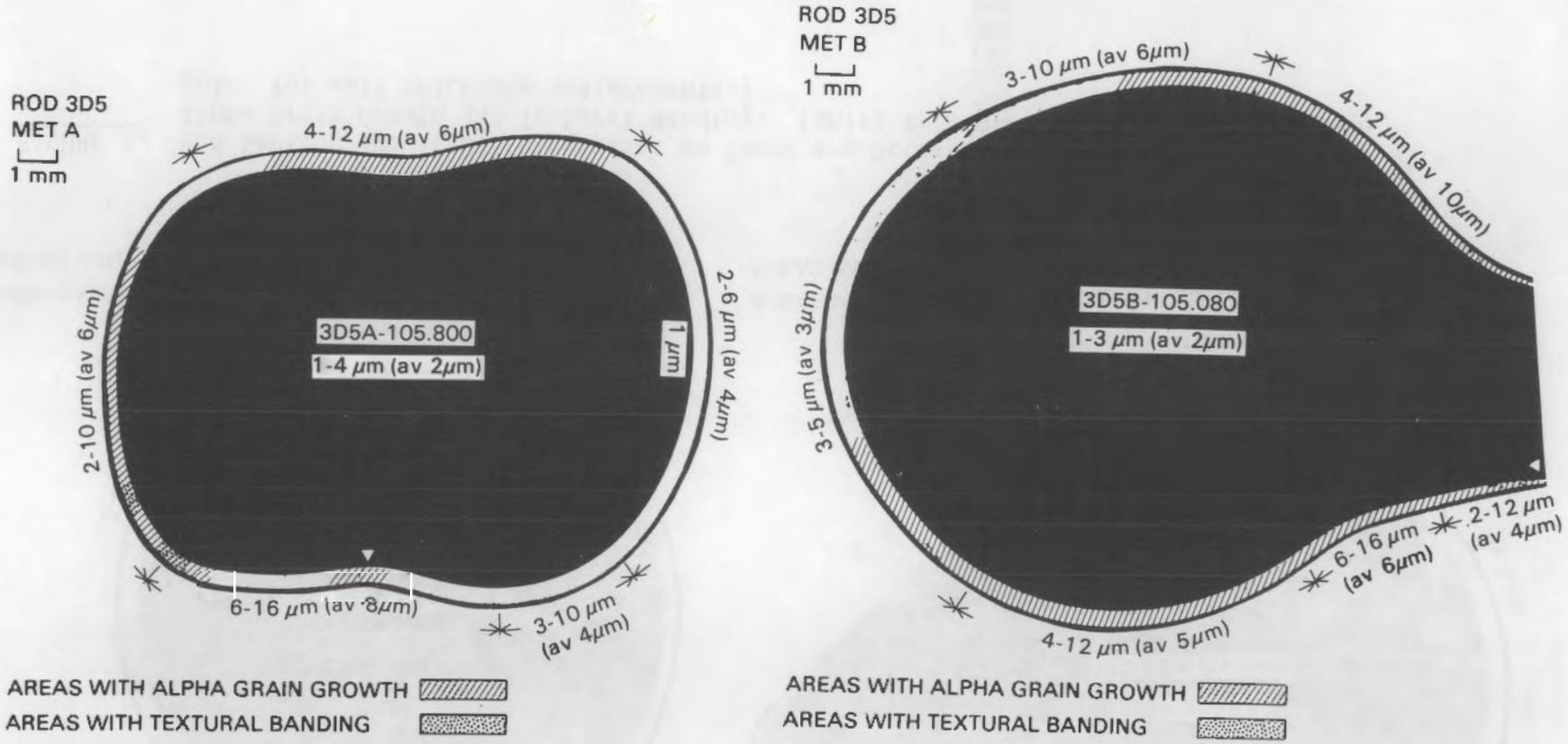

FIGURE 4. Rod Section 3D5, ZrO_2 Thicknesses on Inner and Outer Cladding Surfaces, and Areas with Alpha Grain Growth and Textural Banding. (White triangles indicate the reference point for wall thickness measurements.)

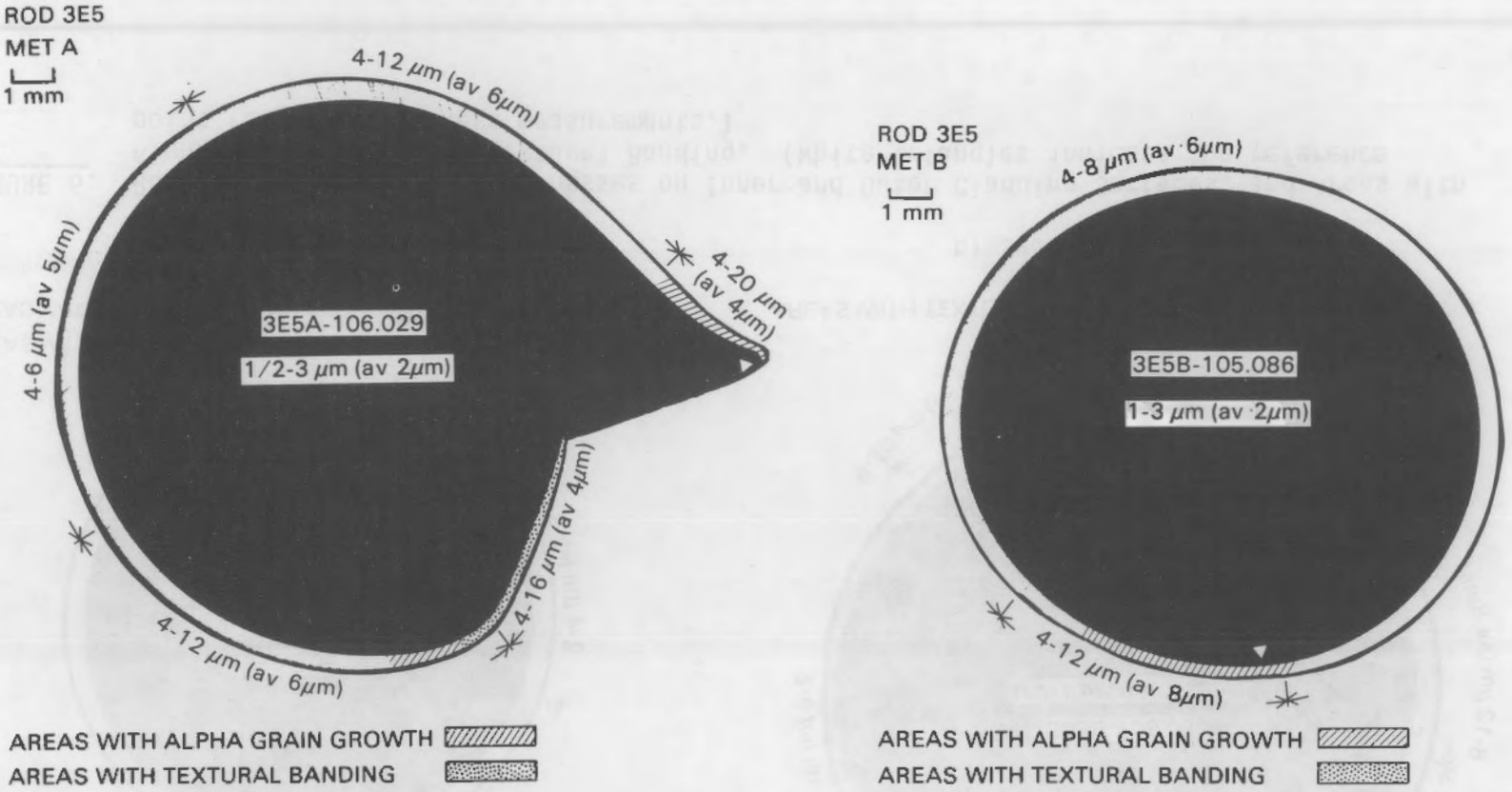

FIGURE 5. Rod Section 3E5, ZrO_2 Thicknesses on Inner and Outer Cladding Surfaces, and Areas with Alpha Grain Growth and Textural Banding. (White triangles indicate the reference point for wall thickness measurements.)

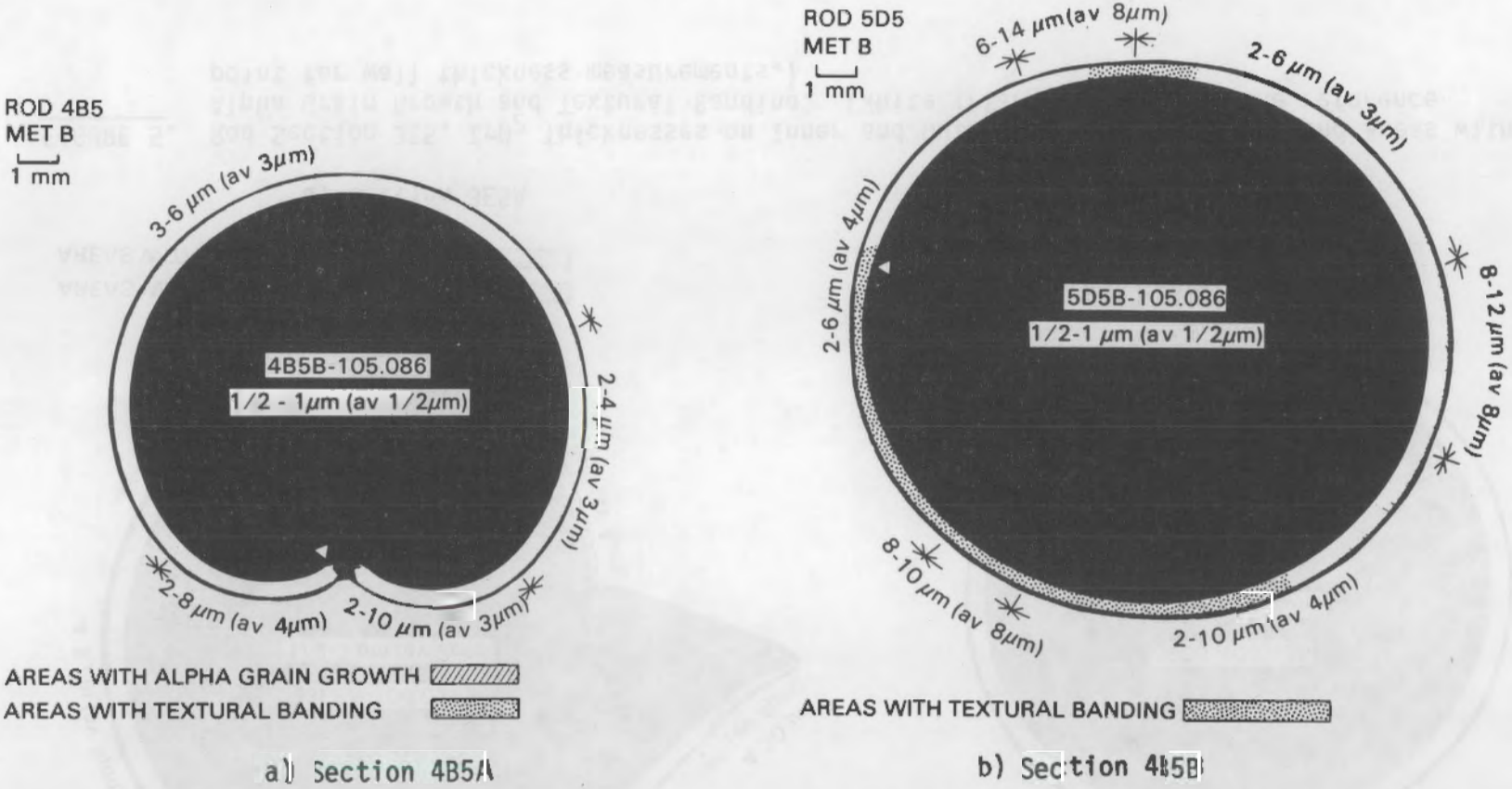

FIGURE 6. Rod Section 4B5, ZrO_2 Thicknesses on Inner and Outer Cladding Surfaces, and Areas with Alpha Grain Growth and Textural Banding. (White triangles indicate the reference point for wall thickness measurements.)

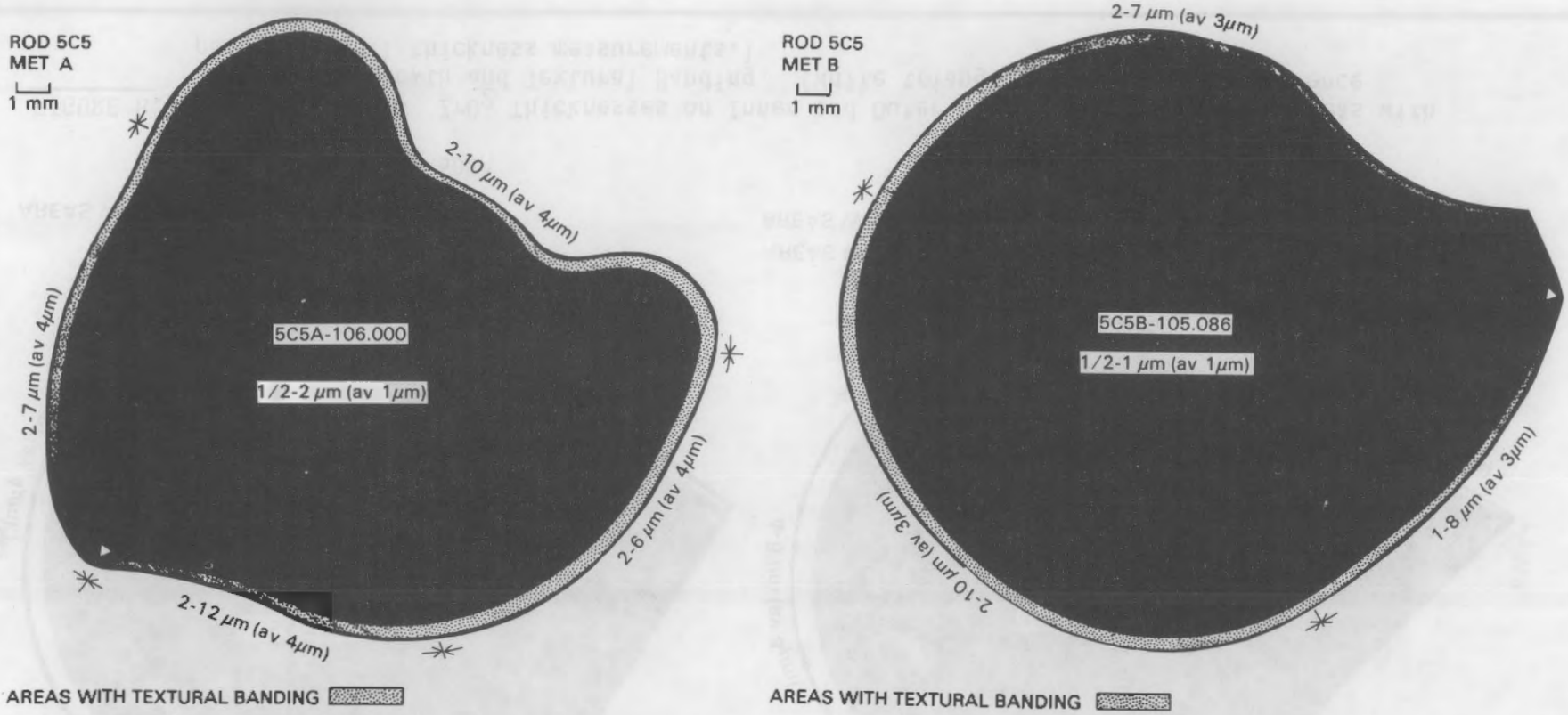

a) Section 5C5A

b) Section 5C5B

FIGURE 7. Rod Section 5C5, ZrO_2 Thicknesses on Inner and Outer Cladding Surfaces, and Areas with Alpha Grain Growth and Textural Banding. (White triangles indicate the reference point for wall thickness measurements.)

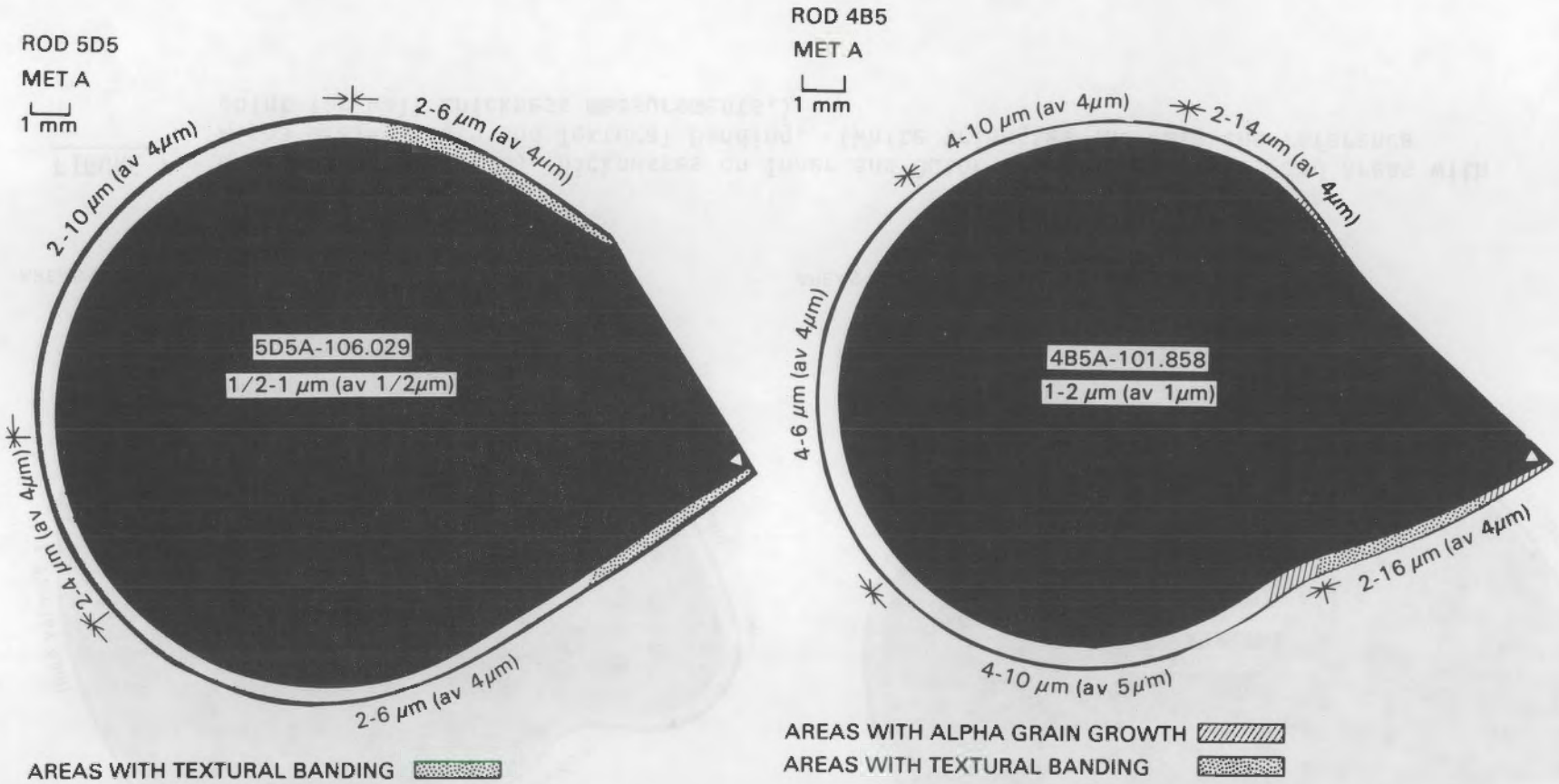

a) Section 5D5A

b) Section 5D5B

FIGURE 8. Rod Section 5D5, ZrO_2 Thicknesses on Inner and Outer Cladding Surfaces, and Areas with Alpha Grain Growth and Textural Banding. (White triangles indicate the reference point for wall thickness measurements.)

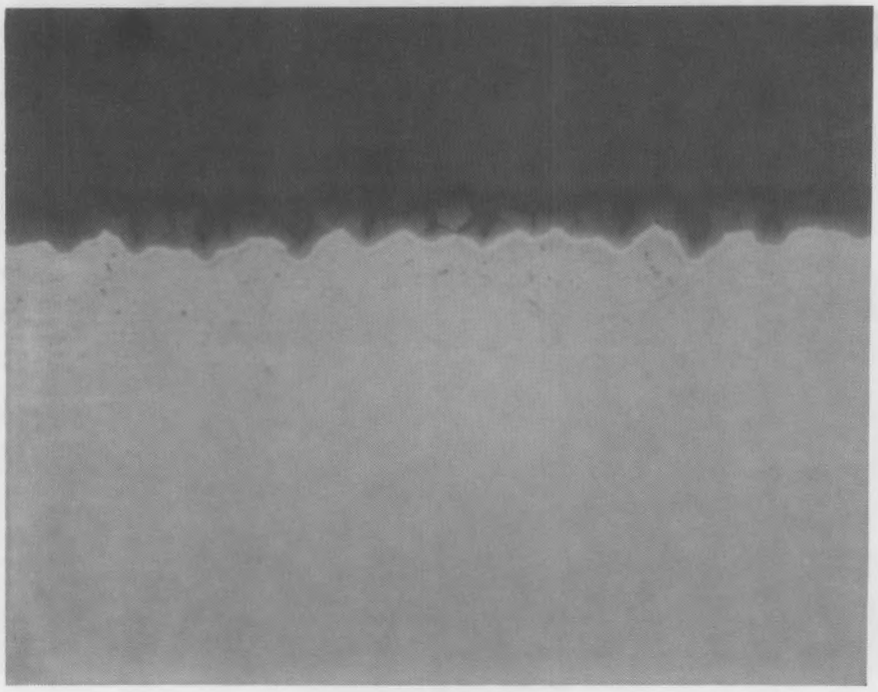

FIGURE 9. ZrO_2 Film and Oxygen-Enriched Layer on Outer Surface of Rod Section 205A (500X)

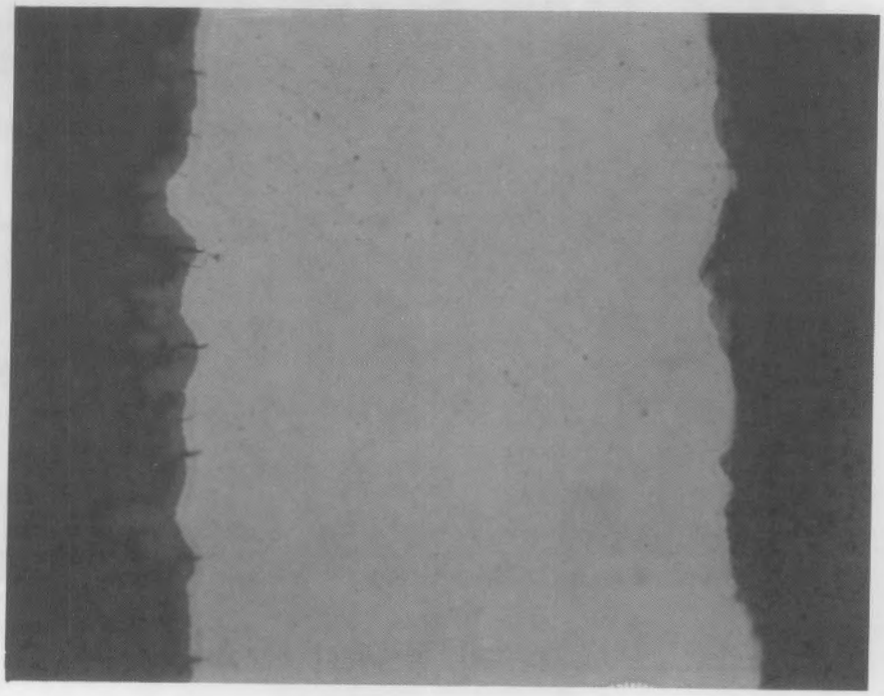

FIGURE 10. Cracks in ZrO_2 Film and Oxygen-Enriched Layer on Inner and Outer Surfaces in the Grossly Distorted Region of Rod Section 205B (500X).

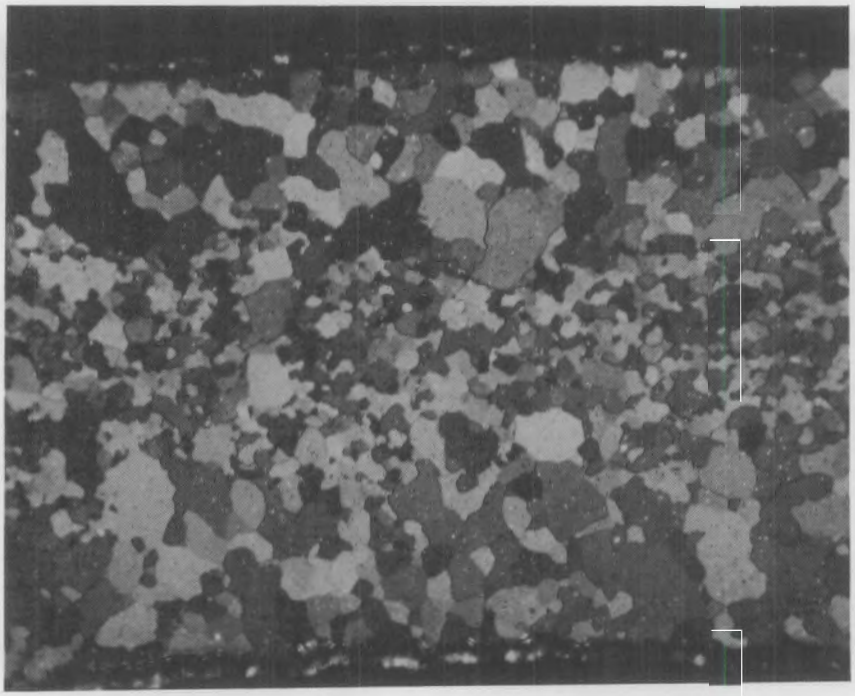

FIGURE 11. Typical Alpha Grain Growth (200X)

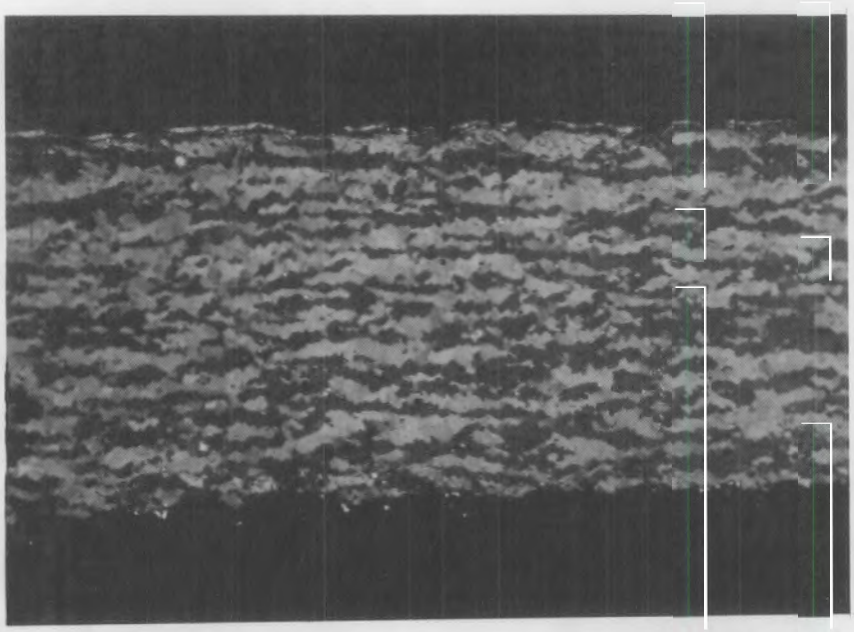

FIGURE 12. Typical Textural Banding (200X)

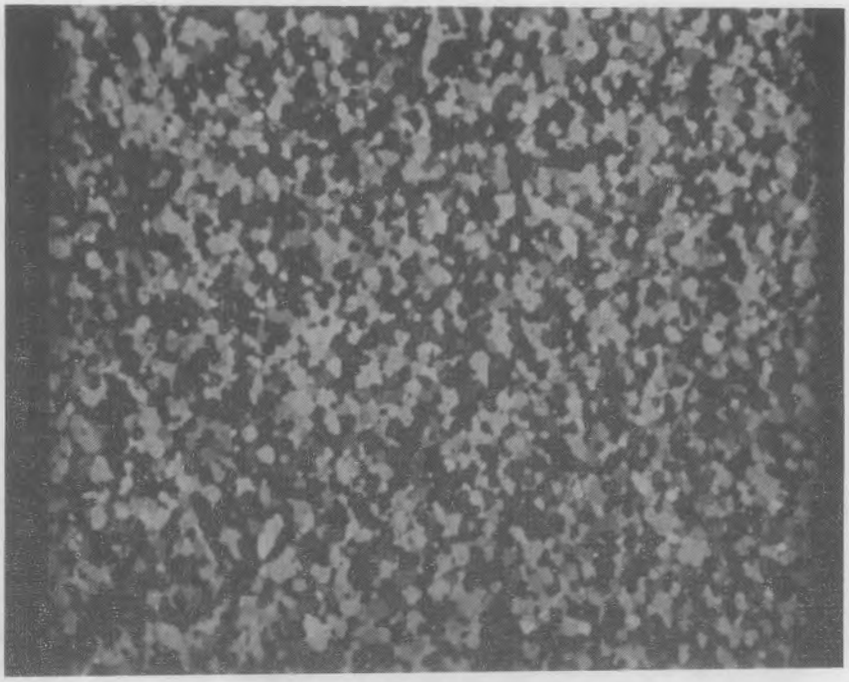

FIGURE 13. Typical Small Alpha-Annealed Grains in Sites Remote from the Rupture Areas (200X)

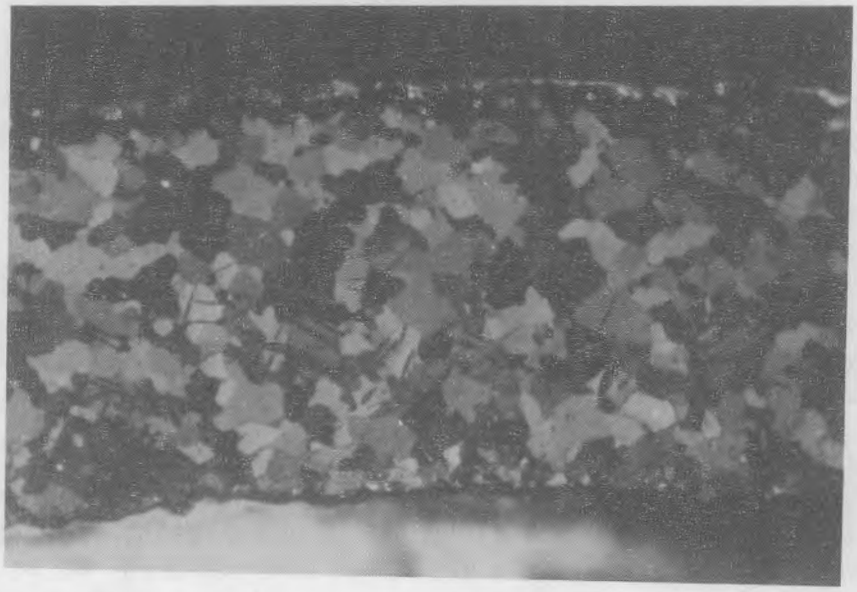

FIGURE 14. Typical Twinning in the Necked-Down Areas of the Cladding (200X)

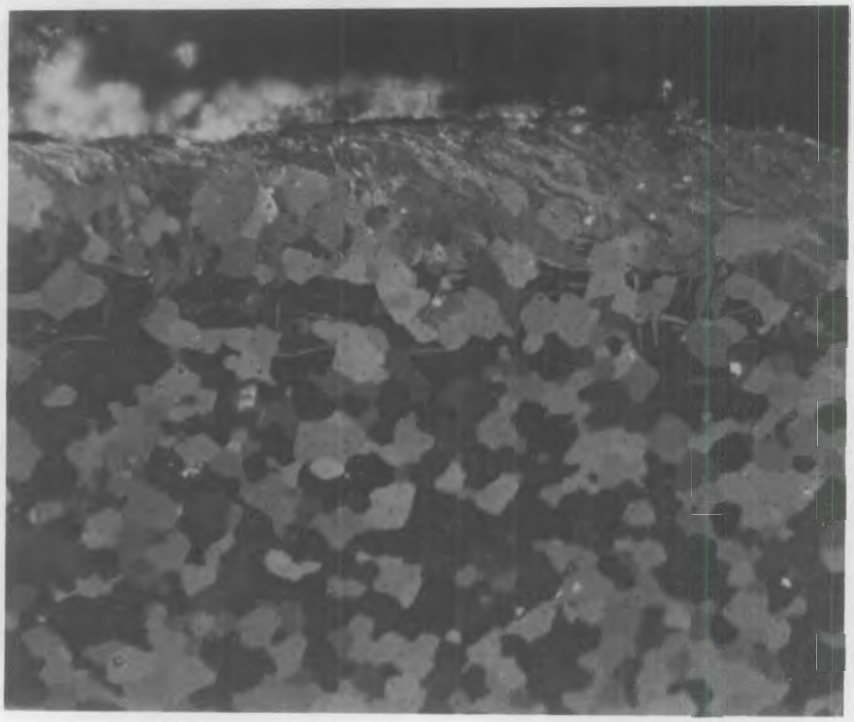

FIGURE 15. Severe Distortion of Grains and Twins on the Outer Surface of Rod Section 3B5A (500X)

Three rods (3D5, 5C5, and 2C5) were sectioned at 1-in. (25.4-mm) intervals, and cladding thickness measurements were made of these cross sections as well. The additional measurements were made to determine whether there was any pattern, such as spiraling, of cladding thinning as a function of radial and axial position. No such pattern was evident. Photographs of the cross sections of Rod 3D5 are presented in Figures 16 through 27, of Rod 5C5 in Figures 28 through 33, and of Rod 2C5 in Figures 34 through 39. The cladding thickness measurements for these three rods are given in Tables 13, 14, and 15, respectively.

The results of the fuel particle size analysis are presented in Table 16, which gives the percentage of the sample weight retained on each size screen. Photographs were taken before and after the size analysis; Figures 40 through 48 show the results from 3B5A. The ballooned and ruptured rod is shown in Figure 40; and the fuel fragments, before sieve shaking, are shown in Figure 41. Figures 42 through 48 show the fuel fragments recovered from each of the six screens and the receiver pan. Only two pellets were still intact after the analysis; both were from rod section 3B5B.

TABLE 5. Thickness of Oxygen-Enriched Layer in the Zircaloy Cladding

Rod Section Identity	Thickness of Oxygen-Enriched Layer, μm	
	Outer Surface	Inner Surface
2O5A	1.5 to 2	1 to 1.5
2O5B	1.5 to 2	1 to 1.5
3B5A	0.5 to 1	0.5 to 1
3B5B	0.5 to 1	0.5 to 1
3O5A	1.5 to 2	1 to 1.5
3D5B	1.5 to 2	1 to 1.5
3E5A	1 to 2	1 to 2
3E5B	1 to 2	1 to 2
4B5A	1 to 2	0.5 to 1
4B5B	1 to 2	0.5 to 1
5C5A	1 to 1.5	0.5 to 1
5C5B	0.5 to 1	0.5 to 1
5D5A	1 to 2	0.5 to 1
5D5B	0.5 to 1	Not visible

TABLE 6. Cladding Thickness Measurements for Rod 2D5[a]

2D5A		2D5B	
Distance from Reference Point,[b] in.	Wall Thickness, in.	Distance from Reference Point,[b] in.	Wall Thickness, in.
0.005	0.0055	0	0.0047
	0.0079		0.0061
	0.0064		0.0095
	0.0070		0.0095
	0.0095		0.0084
	0.0112		0.0093
	0.0123		0.0090
	0.0155		0.0112
	0.0161		0.0128
	0.0173		0.0114
	0.0180		0.0129
	0.0181		0.0139
	0.0186		0.0156
0.050 increments	0.0194	0.050 increments	0.0166
	0.0200		0.0177
	0.0207		0.0189
	0.0211		0.0194
	0.0210		0.0199
	0.0209		0.0202
	0.0206		0.0203
	0.0205		0.0208
	0.0204		0.0209
	0.0200		0.0209
	0.0198		0.0206
	0.0185		0.0198
	0.0173		0.0192
	0.0165		0.0194
	0.0148		0.0184
	0.0138		0.0184
	0.0130		0.0177
	0.0128		0.0172
	0.0113		0.0162
	0.0104		0.0152
	0.0099		0.0142
	0.0070		0.0092
0.002 from fracture tip	0.0024		0.0061

(a) See Figure 2 for reference points.
(b) Direction of travel - clockwise.

TABLE 7. Cladding Thickness Measurements for Rod 3B5[a]

3B5A		3B5B	
Distance from Reference Point,[b] in.	Wall Thickness, in.	Distance from Reference Point,[b] in.	Wall Thickness, in.
0	0.0124	0.0075	0.0039
	0.0123		0.0081
	0.0119		0.0095
	0.0127		0.0112
	0.0128		0.0128
	0.0132		0.0138
	0.0132		0.0147
	0.0135		0.0159
	0.0142		0.0167
	0.0147		0.0176
	0.0149		0.0191
	0.0157		0.0202
	0.0166		0.0211
	0.0173		0.0215
	0.0179	0.050 increments	0.0217
	0.0185		0.0218
	0.0192		0.0209
	0.0194		0.0201
	0.0197		0.0196
0.050 increments	0.0189		0.0198
	0.0204		0.0202
	0.0209		0.0199
	0.0213		0.0189
	0.0214		0.0179
	0.0201		0.0169
	0.0199		0.0147
	0.0197		0.0137
	0.0182		0.0127
	0.0169		0.0113
	0.0158		0.0103
	0.0144		0.0095
	0.0133		0.0084
	0.0131		0.0078
	0.0126		0.0063
	0.0120		0.0039

(a) See Figure 3 for reference points.
(b) Direction of travel - clockwise.

TABLE 8. Cladding Thickness Measurements for Rod 3D5[a]

3D5A		3D5B	
Distance from Reference Point,[b] in.	Wall Thickness, in.	Distance from Reference Point,[b] in.	Wall Thickness, in.
0	0.0149	0.0075	0.0052
	0.0148		0.0093
	0.0147		0.0116
	0.0144		0.0126
	0.0129		0.0130
	0.0125		0.0146
	0.0119		0.0152
	0.0098		0.0159
	0.0109		0.0163
	0.0112		0.0173
	0.0122		0.0174
	0.0146		0.0171
	0.0153		0.0171
	0.0161		0.0170
	0.0174		0.0171
	0.0178		0.0184
	0.0177		0.0192
0.050 increments	0.0184	0.050 increments	0.0196
	0.0185		0.0199
	0.0192		0.0199
	0.0198		0.0199
	0.0199		0.0196
	0.0194		0.0188
	0.0189		0.0181
	0.0177		0.0178
	0.0173		0.0166
	0.0174		0.0162
	0.0173		0.0162
	0.0177		0.0154
	0.0176		0.0139
	0.0169		0.0136
	0.0165		0.0124
	0.0159		0.0109
	0.0152		0.0088
	0.0147	0.020 from fracture tip	0.0065

(a) See Figure 4 for reference points.
(b) Direction of travel - clockwise.

TABLE 9. Cladding Thickness Measurements for Rod 3E5[a]

3E5A		3E5B	
Distance from Reference Point,[b] in.	Wall Thickness, in.	Distance from Reference Point,[b] in.	Wall Thickness, in.
0.0075	0.0033	0	0.0117
↑	0.0070	↑	0.0125
	0.0085		0.0132
	0.0083		0.0135
	0.0095		0.0138
	0.0105		0.0150
	0.0128		0.0160
	0.0155		0.0159
	0.0166		0.0158
	0.0167		0.0167
0.050 increments	0.0171	0.050 increments	0.0170
	0.0183		0.0172
	0.0192		0.0181
	0.0192		0.0186
	0.0202		0.0187
	0.0208		0.0185
	0.0205		0.0190
	0.0205		0.0191
	0.0203		0.0195
	0.0196		0.0202
	0.0198		0.0202
	0.0202		0.0199
	0.0199		0.0198
	0.0195		0.0192
	0.0190		0.0187
	0.0175		0.0194
	0.0172		0.0188
	0.0169		0.0179
	0.0164		0.0170
	0.0162	↓	0.0155
	0.0166	Last step ~0.040	0.0161
	0.0159		
	0.0131		
↓	0.0081		
Last step ~0.035	0.0043		

(a) See Figure 5 for reference points.
(b) Direction of travel - clockwise.

TABLE 10. Cladding Thickness Measurements for Rod 4B5[a]

4B5A		4B5B	
Distance from Reference Point,[b] in.	Wall Thickness, in.	Distance from Reference Point,[b] in.	Wall Thickness, in.
0.010	0.0054	0.015	0.0187
	0.0087		0.0179
	0.0118		0.0180
	0.0135		0.0188
	0.0154		0.0193
	0.0177		0.0192
	0.0187		0.0198
	0.0189		0.0200
	0.0199		0.0199
	0.0204		0.0196
	0.0209		0.0201
	0.0210		0.0204
	0.0211		0.0202
	0.0209		0.0204
	0.0213		0.0206
	0.0209	0.040 increments	0.0207
	0.0207		0.0206
	0.0208		0.0209
	0.0207		0.0209
	0.0205		0.0205
0.050 increments	0.0195		0.0203
	0.0184		0.0204
	0.0179		0.0205
	0.0176		0.0206
	0.0168		0.0203
	0.0166		0.0201
	0.0149		0.0191
	0.0132		0.0188
	0.0098		0.0186
	0.0060		0.0187
0.005 from fracture tip	0.0042		0.0184
			0.0188
		0.013 from fracture tip	0.0202

(a) See Figure 6 for reference points.
(b) Direction of travel - clockwise.

TABLE 11. Cladding Thickness Measurements for Rod 5C5[a]

5C5A		5C5B	
Distance from Reference Point,[b] in.	Wall Thickness, in.	Distance from Reference Point,[b] in.	Wall Thickness, in.
0.010	0.0104	0.010	0.0059
↑	0.0094	↑	0.0082
	0.0109		0.0101
	0.0117		0.0114
	0.0129		0.0119
	0.0128		0.0109
	0.0120		0.0119
	0.0121		0.0127
	0.0123		0.0131
	0.0114		0.0136
	0.0109		0.0131
	0.0100		0.0134
	0.0118		0.0149
	0.0133		0.0152
	0.0142		0.0153
0.050 increments	0.0142		0.0149
	0.0143		0.0144
	0.0135		0.0134
	0.0123		0.0129
	0.0098		0.0139
	0.0072		0.0144
	0.0077		0.0155
	0.0098	0.050	0.0162
	0.0129	increments	0.0163
	0.0143		0.0156
	0.0149		0.0144
	0.0158		0.0138
	0.0166		0.0141
	0.0156		0.0144
	0.0139		0.0155
	0.0134		0.0163
	0.0137		0.0159
	0.0148		0.0151
	0.0159		0.0142
	0.0169		0.0139
	0.0170		0.0119
	0.0161		0.0106
	0.0156		0.0083
	0.0148		0.0094
	0.0133		0.0082

TABLE 11. (Contd)

5C5A		5C5B	
Distance from Reference Point,(b) in.	Wall Thickness, in.	Distance from Reference Point,(b) in.	Wall Thickness, in.
↓	0.0124	↓	0.0076
	0.0117		0.0069
	0.0112	0.0075 from fracture tip	0.0045
	0.0099		
0.0075 from fracture tip	0.0058		

(a) See Figure 7 for reference points.
(b) Direction of travel - clockwise.

TABLE 12. Cladding Thickness Measurements for Rod 5D5[a]

5D5A		5D5B	
Distance from Reference Point,[b] in.	Wall Thickness, in.	Distance from Reference Point,[b] in.	Wall Thickness, in.
0	0.0067	0	0.0087
↑	0.0107	↑	0.0119
	0.0136		0.0144
	0.0133		0.0147
	0.0123		0.0142
	0.0128		0.0149
	0.0142		0.0149
	0.0132		0.0131
	0.0128		0.0115
	0.0139		0.0139
	0.0162		0.0164
	0.0160		0.0174
	0.0155		0.0190
	0.0163		0.0198
	0.0162		0.0199
	0.0139		0.0209
	0.0149		0.0210
0.050 increments	0.0171	0.050 increments	0.0215
	0.0174		0.0210
	0.0187		0.0203
	0.0198		0.0204
	0.0197		0.0191
	0.0202		0.0184
	0.0207		0.0153
	0.0205		0.0134
	0.0210		0.0140
	0.0205		0.0126
	0.0195		0.0114
	0.0197		0.0119
	0.0186		0.0131
	0.0168		0.0119
	0.0154	↓	
↓	0.0146		
0.0075 from fracture tip	0.0104		
	0.0067		

(a) See Figure 8 for reference points.
(b) Direction of travel - clockwise.

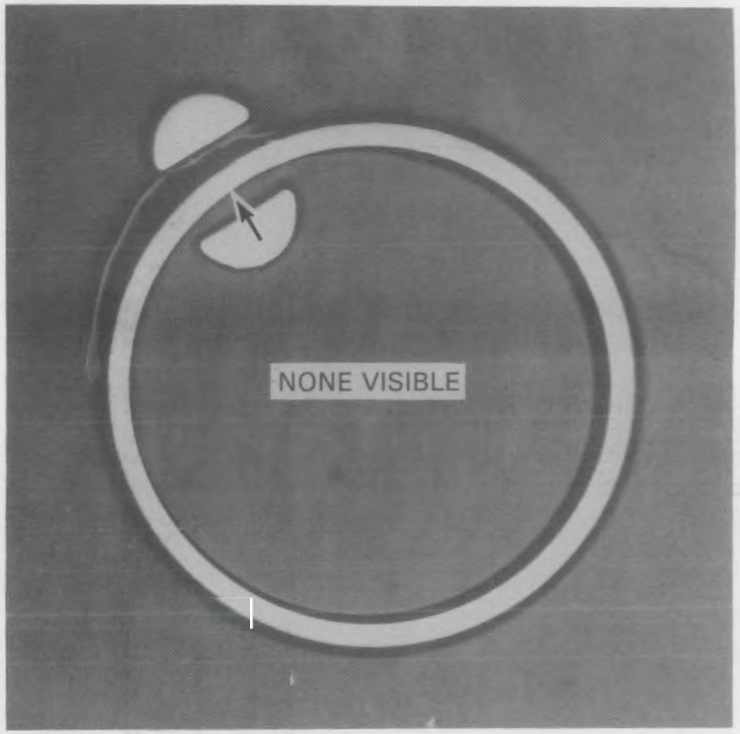

FIGURE 16. Rod Section 3D5-1, ZrO_2 Thickness (μm) on Inner and Outer Cladding Surfaces are as Shown. (Arrow indicates the reference point for wall thickness measurements.)

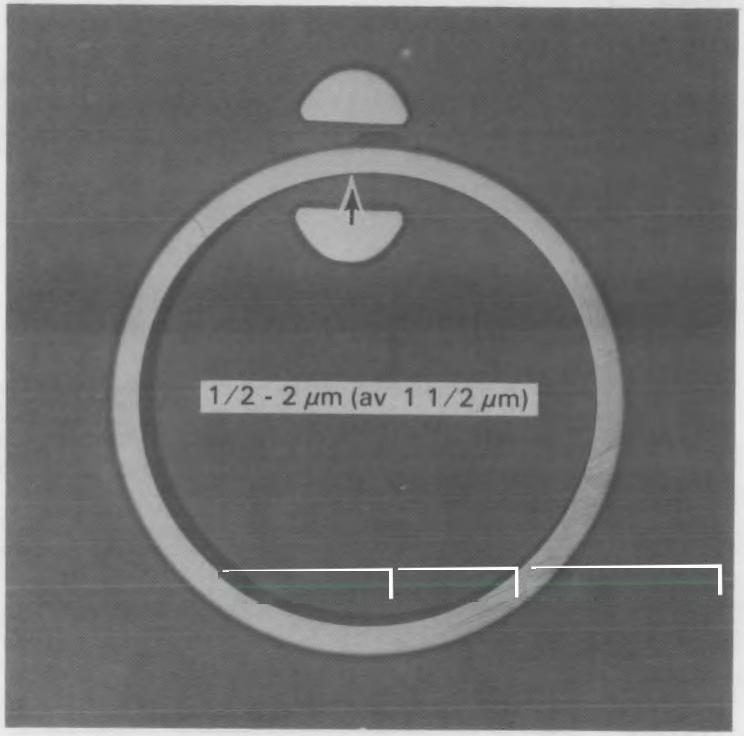

FIGURE 17. Rod Section 3D5-7, ZrO_2 Thickness (μm) on Inner and Outer Cladding Surfaces are as Shown. (Arrow indicates the reference point for wall thickness measurements.)

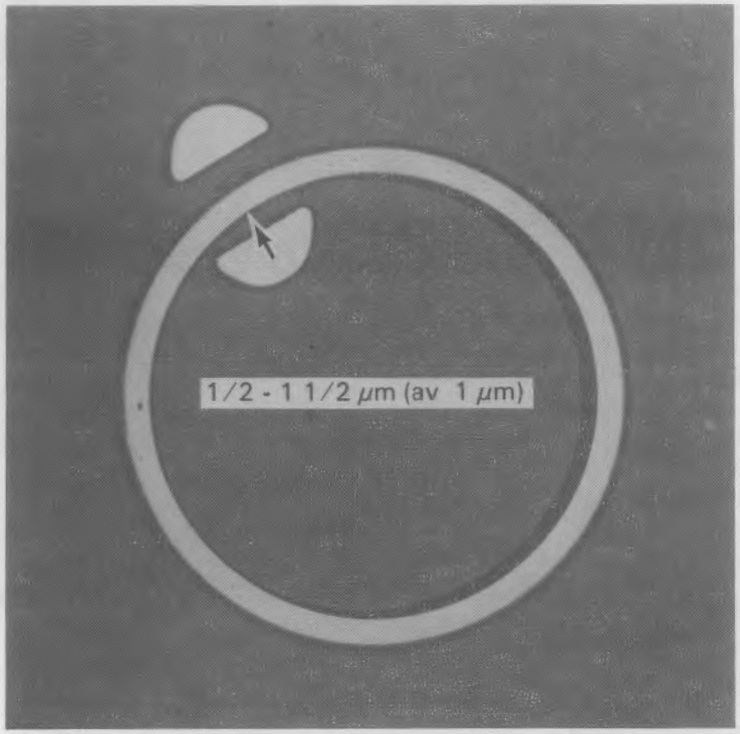

FIGURE 18. Rod Section 3D5-6, ZrO_2 Thickness (μm) on Inner and Outer Cladding Surfaces are as Shown. (Arrow indicates the reference point for wall thickness measurements.)

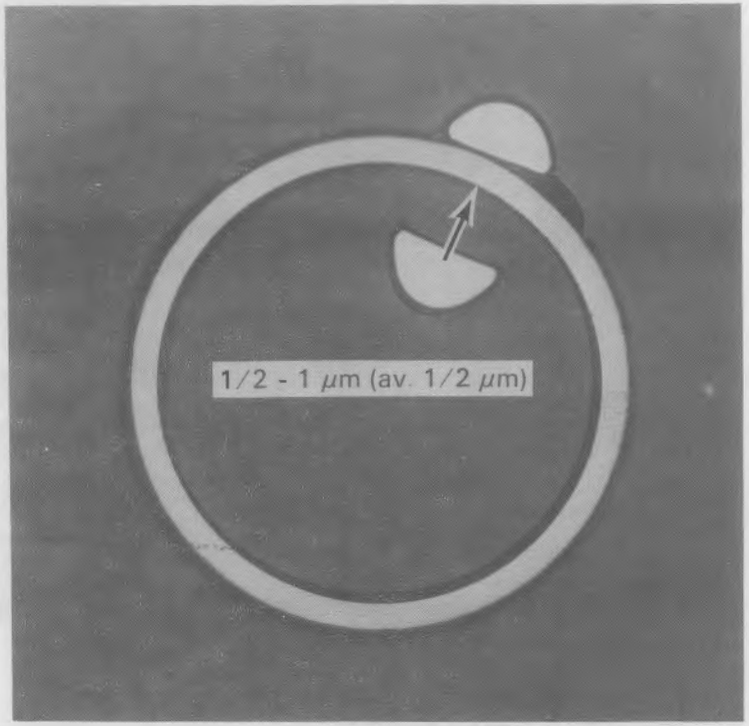

FIGURE 19. Rod Section 3D5-5, ZrO_2 Thickness (μm) on Inner and Outer Cladding Surfaces are as Shown. (Arrow indicates the reference point for wall thickness measurements.)

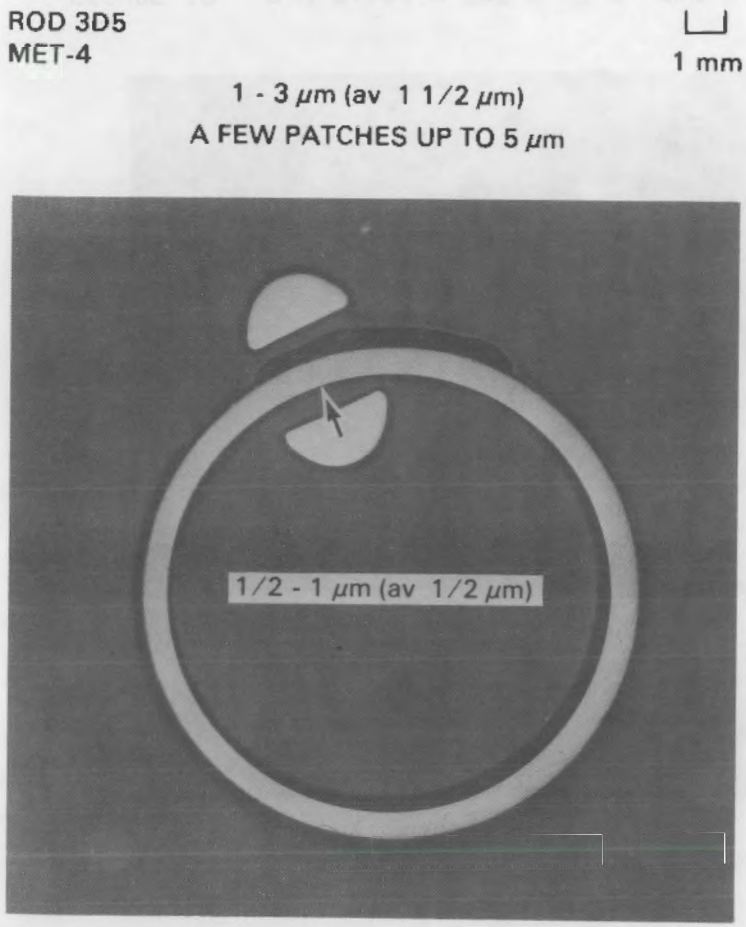

FIGURE 20. Rod Section 3D5-4, ZrO_2 Thickness (μm) on Inner and Outer Cladding Surfaces are as Shown. (Arrow indicates the reference point for wall thickness measurements.)

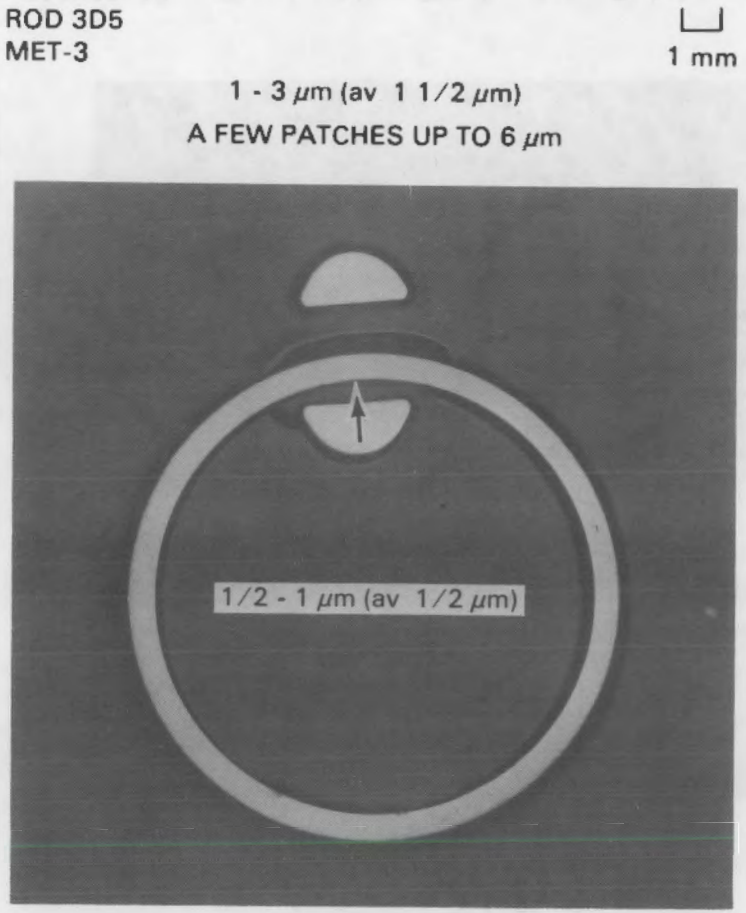

FIGURE 21. Rod Section 3D5-3, ZrO_2 Thickness (μm) on Inner and Outer Cladding Surfaces are as Shown. (Arrow indicates the reference point for wall thickness measurements.)

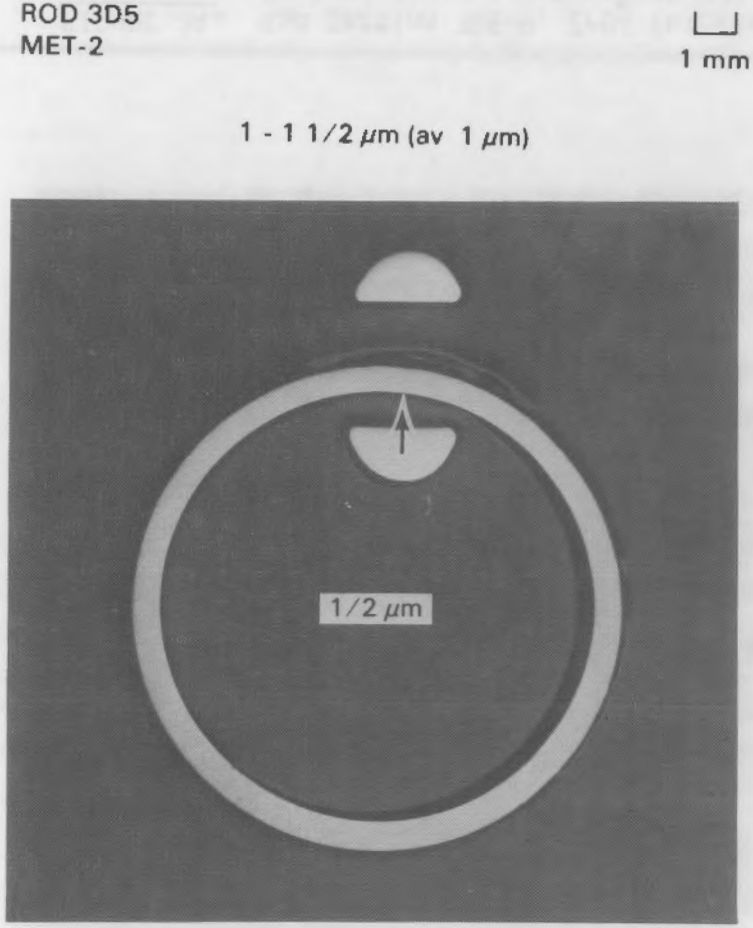

FIGURE 22. Rod Section 3D5-2, ZrO_2 Thickness (μm) on Inner and Outer Cladding Surfaces are as Shown. (Arrow indicates the reference point for wall thickness measurements.)

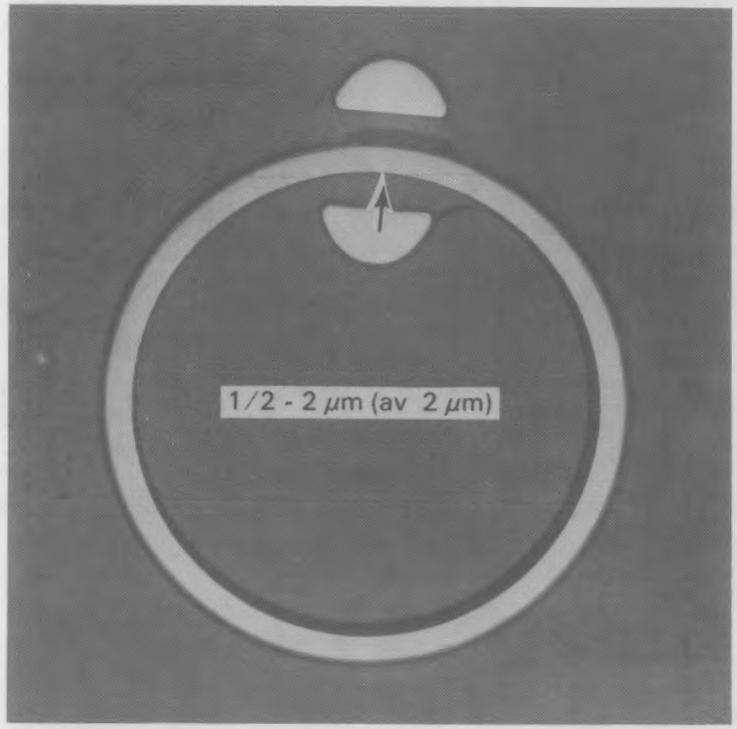

FIGURE 23. Rod Section 3D5-8, ZrO_2 Thickness (μm) on Inner and Outer Cladding Surfaces are as Shown. (Arrow indicates the reference point for wall thickness measurements.)

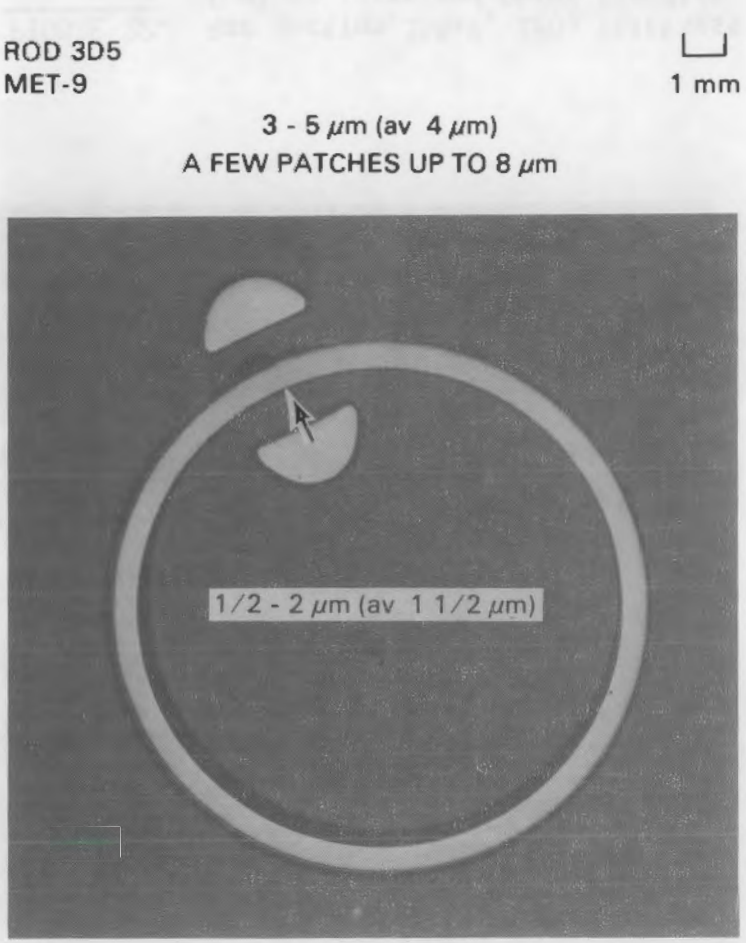

FIGURE 24. Rod Section 3D5-9, ZrO_2 Thickness (μm) on Inner and Outer Cladding Surfaces are as Shown. (Arrow indicates the reference point for wall thickness measurements.)

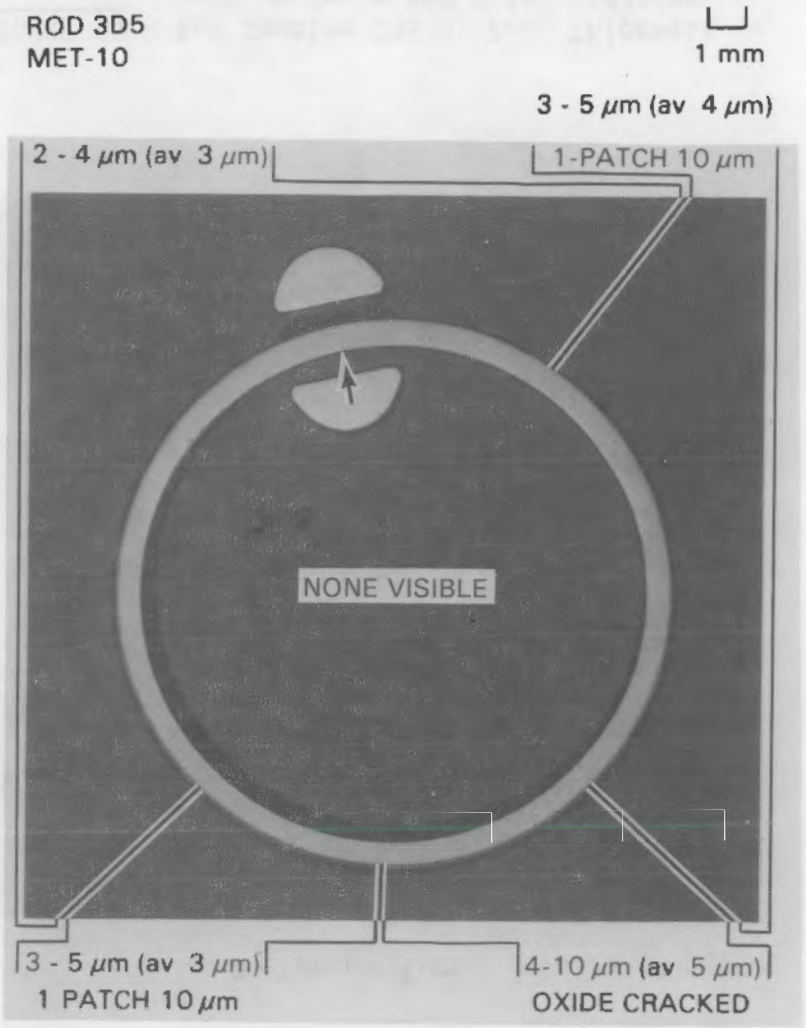

FIGURE 25. Rod Section 3D5-10, ZrO_2 Thickness (μm) on Inner and Outer Cladding Surfaces are as Shown. (Arrow indicates the reference point for wall thickness measurements.)

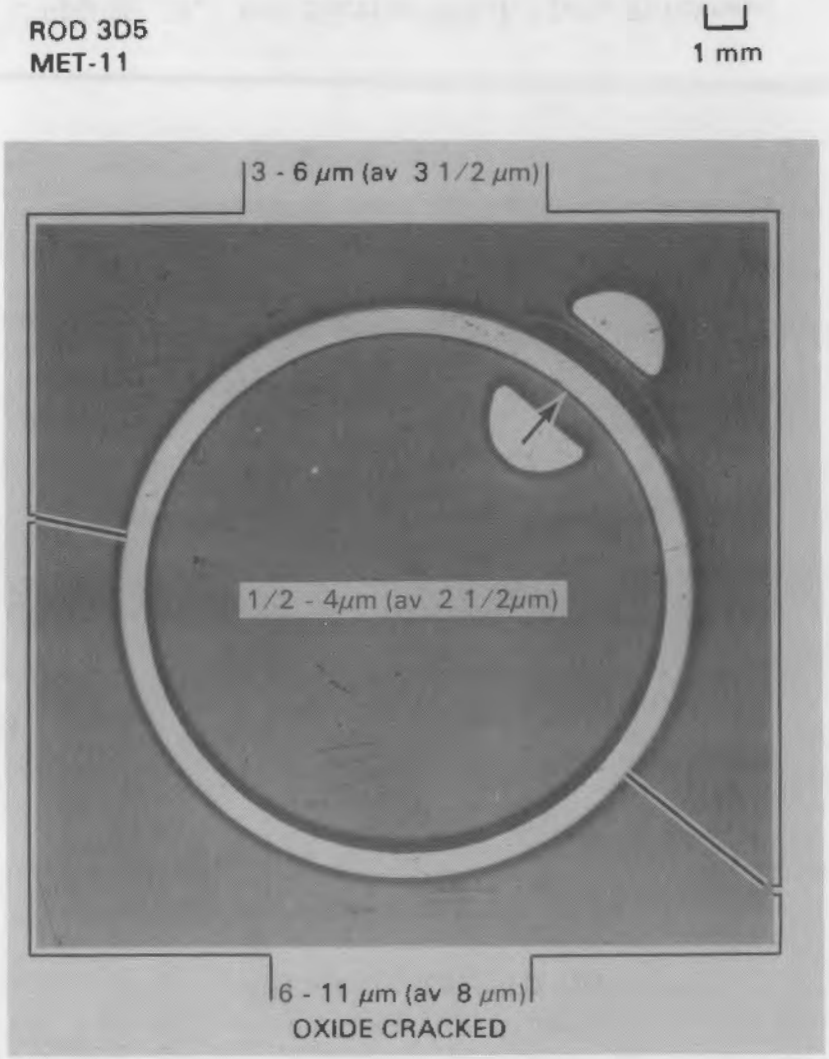

FIGURE 26. Rod Section 3D5-11, ZrO_2 Thickness (μm) on Inner and Outer Cladding Surfaces are as Shown. (Arrow indicates the reference point for wall thickness measurements.)

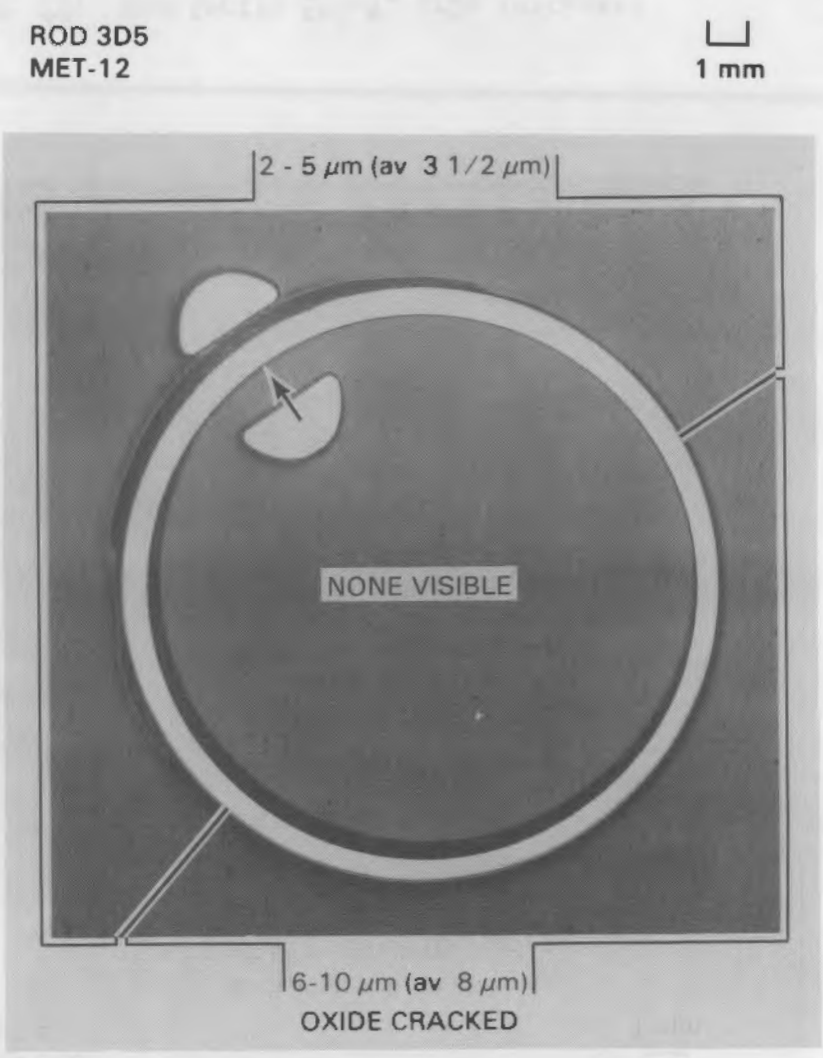

FIGURE 27. Rod Section 3D5-12, ZrO_2 Thickness (μm) on Inner and Outer Cladding Surfaces are as Shown. (Arrow indicates the reference point for wall thickness measurements.)

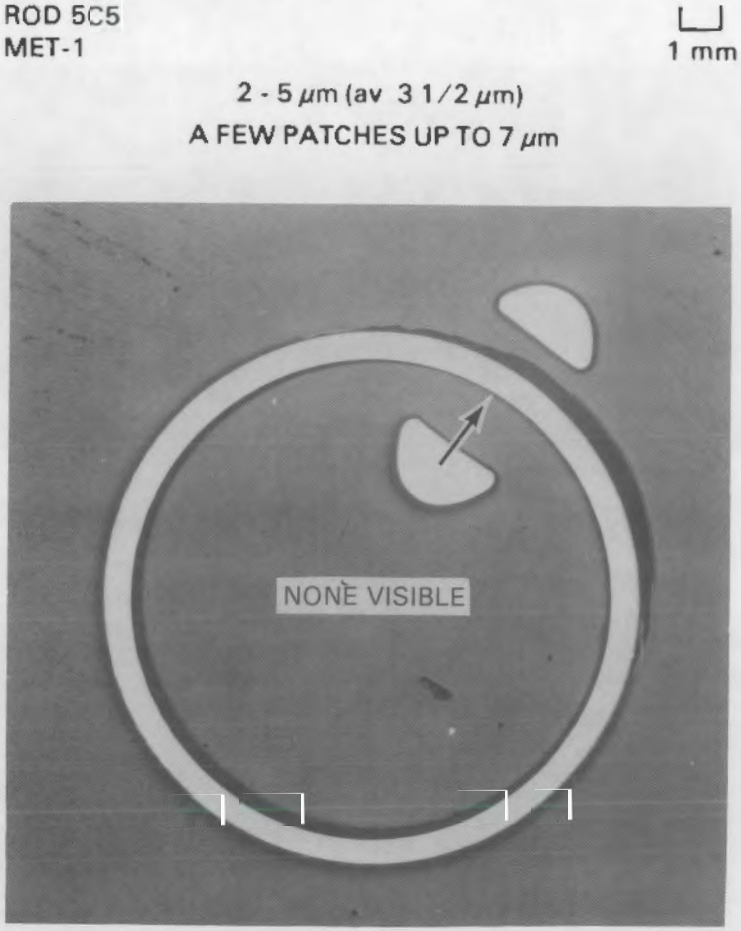

FIGURE 28. Rod Section 5C5-1, ZrO_2 Thickness (μm) on Inner and Outer Cladding Surfaces are as Shown. (Arrow indicates the reference point for wall thickness measurements.)

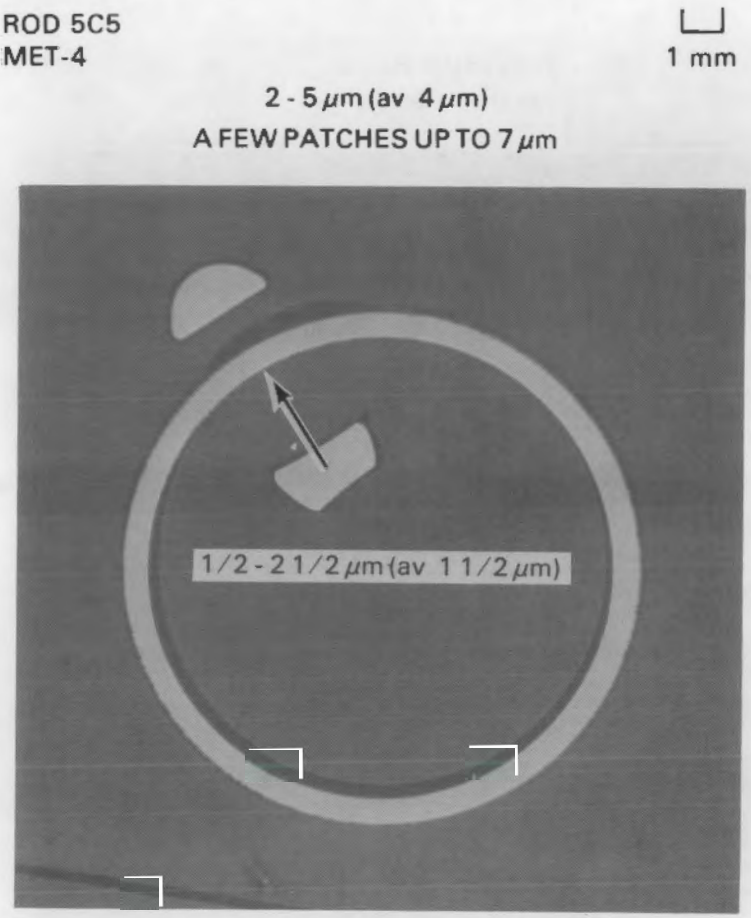

FIGURE 29. Rod Sectin 5C5-4, ZrO_2 Thickness (μm) on Inner and Outer Cladding Surfaces are as Shown. (Arrow indicates the reference point for wall thickness measurements.)

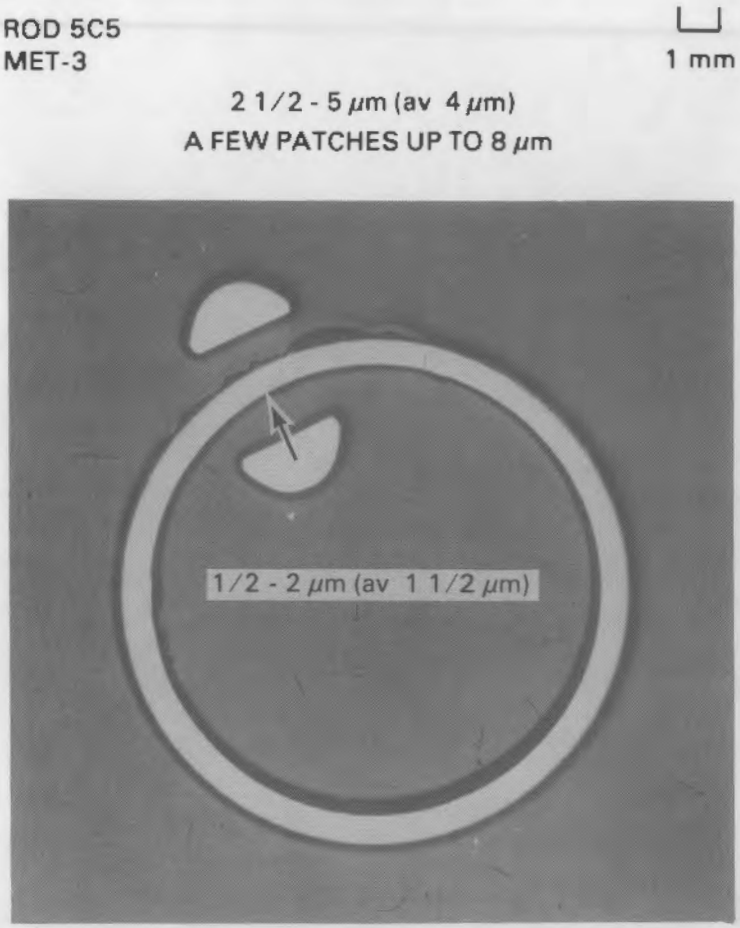

FIGURE 30. Rod Section 5C5-3, ZrO_2 Thickness (μm) on Inner and Outer Cladding Surfaces are as Shown. (Arrow indicates the reference point for wall thickness measurements.)

FIGURE 31. Rod Section 5C5-2, ZrO_2 Thickness (μm) on Inner and Outer Cladding Surfaces are as Shown. (Arrow indicates the reference point for wall thickness measurements.)

ROD 5C5
MET-5

1 mm

3 - 5 μm (av 4 μm)
A FEW PATCHES UP TO 10 μm

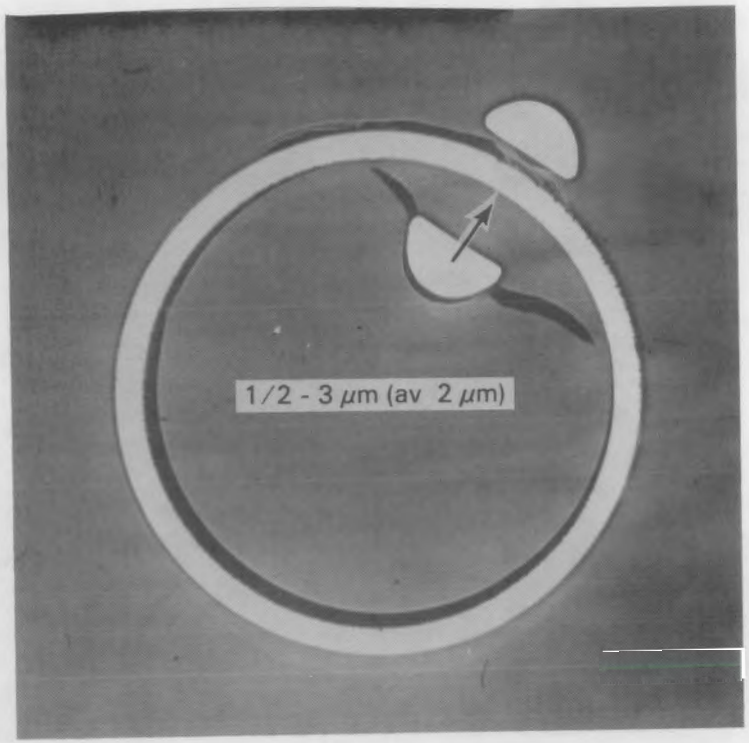

FIGURE 32. Rod Section 5C5-5, ZrO_2 Thickness (μm) on Inner and Outer Cladding Surfaces are as Shown. (Arrow indicates the reference point for wall thickness measurements.)

ROD 5C5
MET-6

1 mm

3 - 5 μm (av 4 μm)
A FEW PATCHES UP TO 8 μm

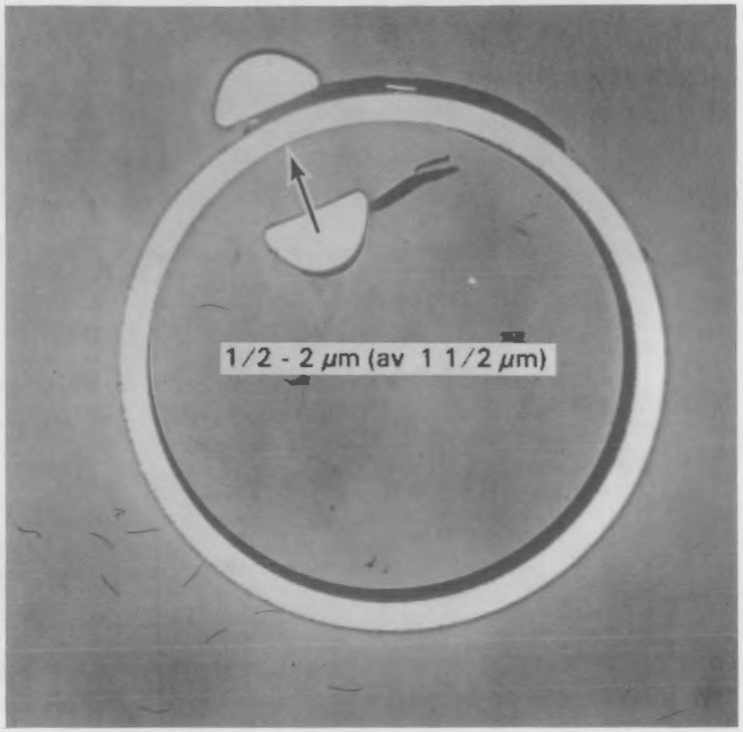

FIGURE 33. Rod Section 5C5-6, ZrO_2 Thickness (μm) on Inner and Outer Cladding Surfaces are as Shown. (Arrow indicates the reference point for wall thickness measurements.)

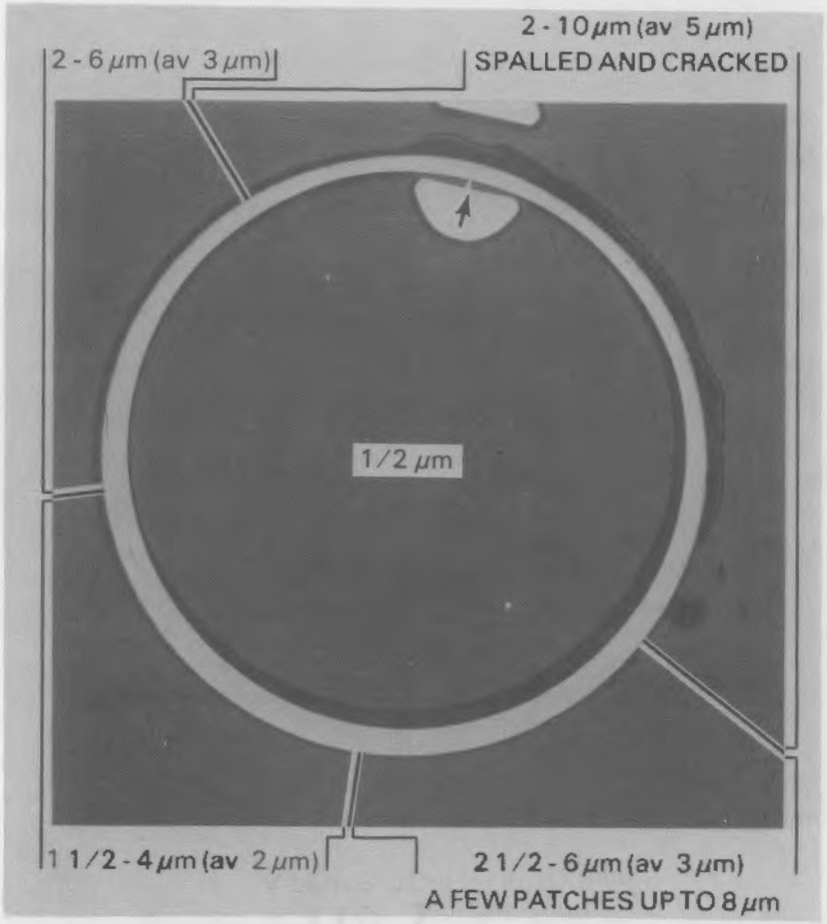

FIGURE 34. Rod Section 2C5-1, ZrO_2 Thickness (μm) on Inner and Outer Cladding Surfaces are as Shown. (Arrow indicates the reference point for wall thickness measurements.)

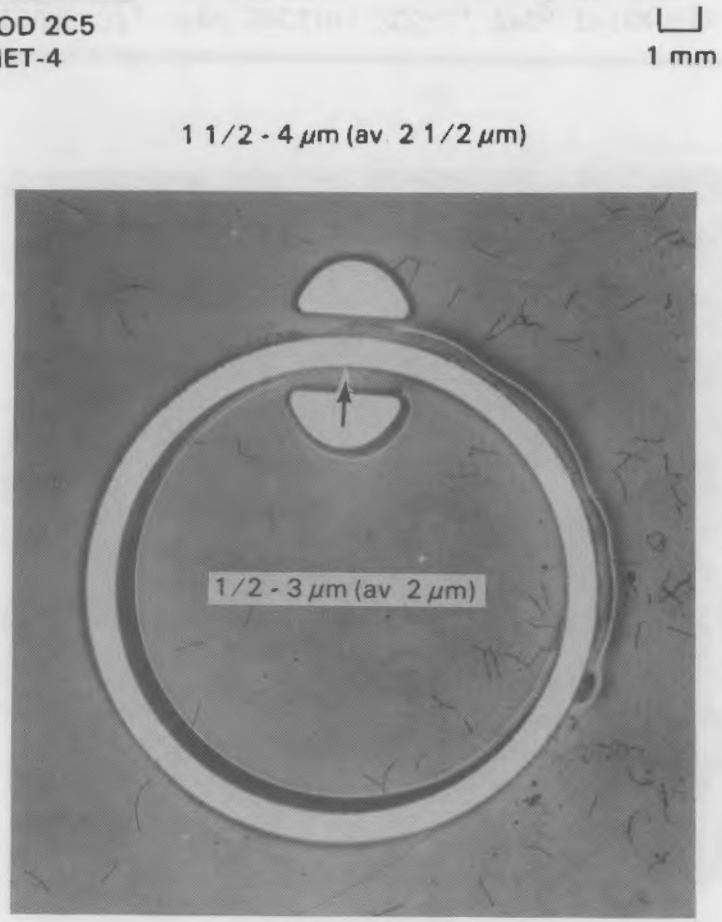

FIGURE 35. Rod Section 2C5-4, ZrO_2 Thickness (μm) on Inner and Outer Cladding Surfaces are as Shown. (Arrow indicates the reference point for for wall thickness measurements.)

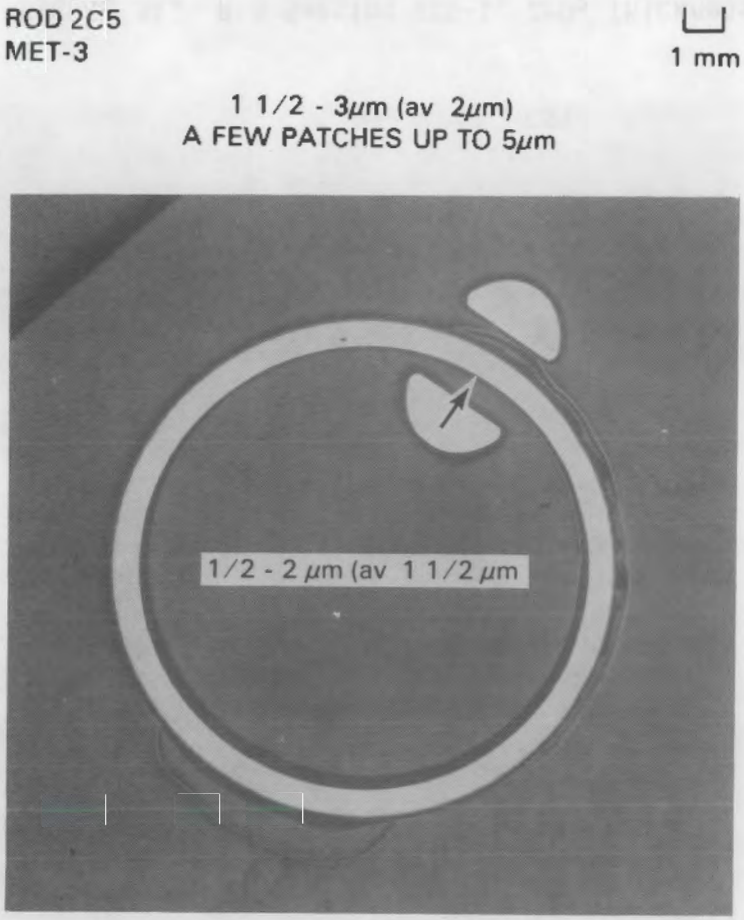

FIGURE 36. Rod Section 2C5-3, ZrO_2 Thickness (μm) on Inner and Outer Cladding Surfaces are as Shown. (Arrow indicates the reference point for wall thickness measurements.)

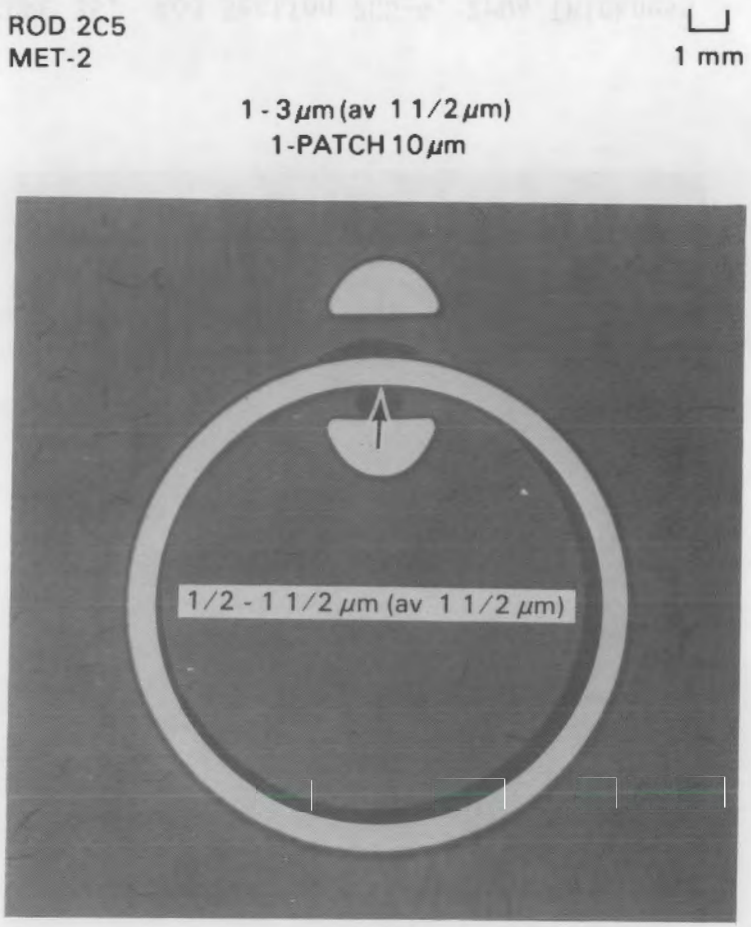

FIGURE 37. Rod Section 2C5-2, ZrO_2 Thickness (μm) on Inner and Outer Cladding Surfaces are as Shown. (Arrow indicates the reference point for wall thickness measurements.)

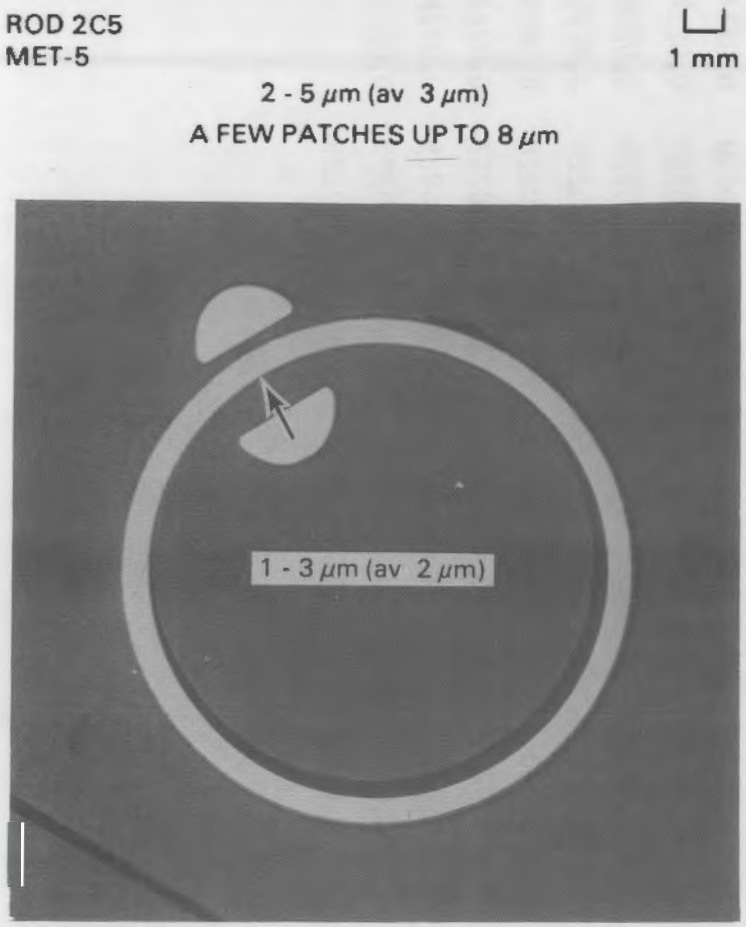

FIGURE 38. Rod Section 2C5-5, ZrO_2 Thickness (μm) on Inner and Outer Cladding Surfaces are as Shown. (Arrow indicates the reference point for wall thickness measurements.)

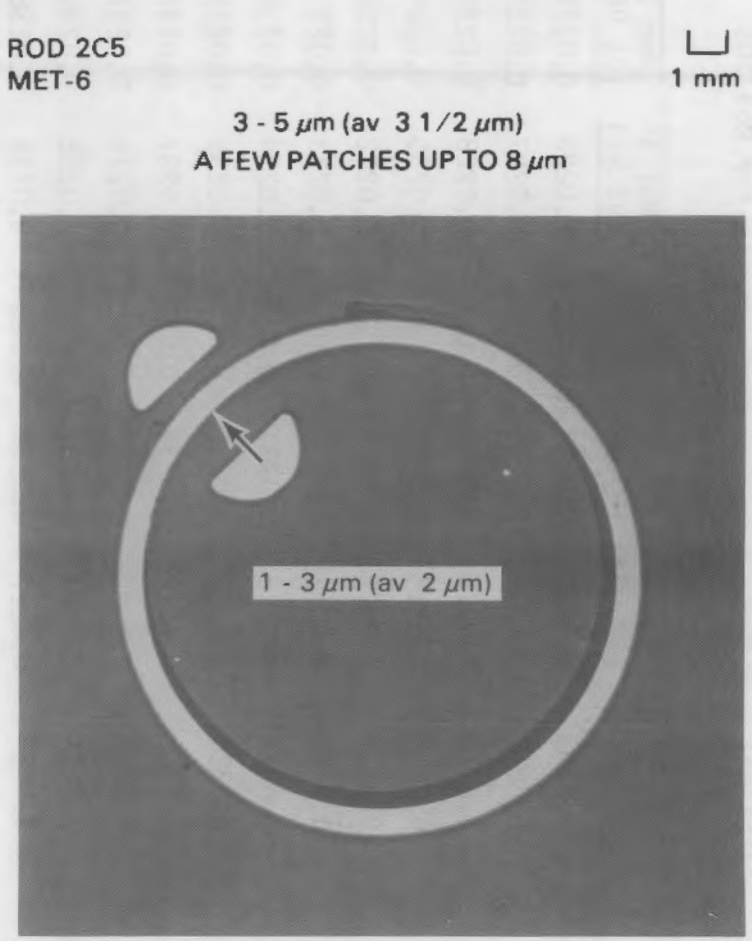

FIGURE 39. Rod Section 2C5-6, ZrO_2 Thickness (μm) on Inner and Outer Cladding Surfaces are as Shown. (Arrow indicates the reference point for wall thickness measurements.)

TABLE 13. Additional Cladding Thickness Measurements for Rod 3D5

Distance from Reference Point,[a] in.	Wall Thickness, in.					
	Met 1 (84.82)[b]	Met 7 (92.98)	Met 6 (93.98)	Met 5 (94.98)	Met 4 (95.98)	Met 3 (96.98)
0	0.0203	0.0214	0.0219	0.0224	0.0223	0.0225
↑	0.0210	0.0217	0.0223	0.0224	0.0227	0.0228
	0.0210	0.0215	0.0225	0.0224	0.0228	0.0228
	0.0214	0.0218	0.0229	0.0222	0.0230	0.0229
	0.0219	0.0218	0.0228	0.0224	0.0232	0.0232
	0.0222	0.0217	0.0230	0.0222	0.0233	0.0232
	0.0224	0.0219	0.0231	0.0224	0.0234	0.0235
	0.0226	0.0220	0.0233	0.0226	0.0235	0.0235
	0.0226	0.0222	0.0233	0.0226	0.0237	0.0237
	0.0227	0.0222	0.0232	0.0229	0.0235	0.0237
0.050 increments	0.0224	0.0224	0.0232	0.0231	0.0235	0.0239
	0.0224	0.0227	0.0230	0.0234	0.0234	0.0238
	0.0223	0.0227	0.0229	0.0233	0.0233	0.0238
	0.0222	0.0230	0.0229	0.0237	0.0233	0.0237
	0.0219	0.0230	0.0228	0.0233	0.0230	0.0234
	0.0216	0.0231	0.0225	0.0233	0.0229	0.0232
	0.0214	0.0229	0.0224	0.0234	0.0228	0.0230
	0.0208	0.0230	0.0222	0.0234	0.0229	0.0229
	0.0206	0.0228	0.0221	0.0235	0.0228	0.0228
	0.0201	0.0226	0.0221	0.0230	0.0227	0.0227
	0.0200	0.0224	0.0220	0.0230	0.0225	0.0226
	0.0197	0.0220	0.0223	0.0227	0.0223	0.0228
	0.0199	0.0220	0.0221	0.0227	0.0226	
↓	0.0201					

TABLE 13. (Contd)

Distance from Reference Point,[a] in.	Wall Thickness, in.					
	Met 2 (97.98)	Met 8 (98.98)	Met 9 (99.98)	Met 10 (100.98)	Met 11 (101.98)	Met 12 (102.98)
0	0.0229	0.0209	0.0207	0.0204	0.0211	0.0210
	0.0232	0.0214	0.0210	0.0204	0.0212	0.0209
	0.0230	0.0212	0.0209	0.0206	0.0205	0.0208
	0.0233	0.0213	0.0207	0.0201	0.0205	0.0206
	0.0235	0.0211	0.0205	0.0203	0.0200	0.0205
	0.0238	0.0212	0.0205	0.0202	0.0198	0.0202
	0.0238	0.0213	0.0204	0.0199	0.0198	0.0191
	0.0239	0.0216	0.0209	0.0200	0.0191	0.0188
	0.0239	0.0218	0.0209	0.0197	0.0191	0.0169
	0.0240	0.0217	0.0209	0.0200	0.0189	0.0160
	0.0241	0.0220	0.0211	0.0203	0.0189	0.0157
	0.0241	0.0221	0.0212	0.0203	0.0189	0.0156
0.050 increments	0.0240	0.0223	0.0214	0.0205	0.0184	0.0155
	0.0238	0.0225	0.0213	0.0202	0.0182	0.0159
	0.0238	0.0223	0.0217	0.0204	0.0180	0.0165
	0.0236	0.0225	0.0217	0.0204	0.0179	0.0168
	0.0236	0.0222	0.0218	0.0204	0.0183	0.0175
	0.0234	0.0225	0.0219	0.0207	0.0185	0.0186
	0.0233	0.0224	0.0216	0.0205	0.0183	0.0188
	0.0233	0.0222	0.0216	0.0206	0.0191	0.0190
	0.0230	0.0220	0.0217	0.0206	0.0197	0.0192
	0.0229	0.0215	0.0214	0.0207	0.0204	0.0199
	0.0229	0.0215	0.0212	0.0207	0.0207	0.0200
			0.0207	0.0207	0.0206	0.0202
				0.0207	0.0209	0.0206

(a) Direction of travel was clockwise for all samples. See Figures 16 through 27 for reference points; 0 reference point was picked at random and a scribe line was made along the length of the rod section before mets were cut.

(b) Z-location requested (inches from bottom of rod). Mets were numbered chronologically, as they were made and measured, rather than with respect to position along the rod.

TABLE 14. Additional Cladding Thickness Measurements for Rod 5C5

Distance from Reference Point,[a] in.	Wall Thickness, in.					
	Met 1 (84.82)[b]	Met 4 (95.98)	Met 3 (96.98)	Met 2 (97.98)	Met 5 (98.98)	Met 6 (99.98)
0	0.0218	0.0210	0.0218	0.0229	0.0204	0.0188
↓	0.0219	0.0215	0.0217	0.0226	0.0204	0.0197
	0.0221	0.0222	0.0217	0.0224	0.0205	0.0203
	0.0223	0.0222	0.0217	0.0224	0.0208	0.0206
	0.0227	0.0225	0.0216	0.0222	0.0208	0.0208
	0.0225	0.0215	0.0214	0.0219	0.0205	0.0208
	0.0220	0.0228	0.0211	0.0219	0.0206	0.0214
	0.0218	0.0232	0.0216	0.0221	0.0211	0.0221
	0.0216	0.0233	0.0220	0.0221	0.0216	0.0223
	0.0214	0.0230	0.0222	0.0221	0.0217	0.0221
	0.0212	0.0229	0.0220	0.0221	0.0216	0.0221
0.050 increments	0.0206	0.0230	0.0224	0.0223	0.0214	0.0221
↓	0.0204	0.0227	0.0231	0.0228	0.0222	0.0224
	0.0206	0.0223	0.0233	0.0229	0.0224	0.0221
	0.0207	0.0220	0.0232	0.0229	0.0226	0.0218
	0.0205	0.0221	0.0232	0.0233	0.0223	0.0216
	0.0204	0.0219	0.0236	0.0239	0.0224	0.0217
	0.0207	0.0215	0.0237	0.0236	0.0226	0.0215
	0.0209	0.0212	0.0234	0.0236	0.0226	0.0210
	0.0212	0.0211	0.0233	0.0235	0.0223	0.0209
	0.0212	0.0210	0.0229	0.0235	0.0219	0.0209
	0.0210	0.0214	0.0229		0.0217	0.0203
	0.0214	0.0212	0.0226		0.0216	0.0202
	0.0219	0.0211			0.0212	0.0198
	0.0220					0.0192

(a) Direction of travel was clockwise for all samples. See Figures 28 through 33 for reference points; 0 reference point was made at random and a scribe line was made along the length of the rod section before mets were cut.

(b) Z-location requested (inches from bottom of rod). Mets were numbered chronologically, as they were made and measured, rather than with respect to position along the rod.

TABLE 15. Additional Cladding Thickness Measurements for Rod 2C5

Distance from Reference Point,[a] in.	Wall Thickness, in.					
	Met 1 (84.82)[b]	Met 4 (95.98)	Met 3 (96.98)	Met 2 (97.98)	Met 5 (98.98)	Met 6 (99.98)
0	0.0149	0.0222	0.0221	0.0224	0.0218	0.0204
↑	0.0142	0.0222	0.0221	0.0226	0.0216	0.0207
	0.0140	0.0219	0.0220	0.0226	0.0216	0.0207
	0.0145	0.0218	0.0217	0.0226	0.0212	0.0207
	0.0150	0.0215	0.0220	0.0222	0.0216	0.0211
	0.0143	0.0218	0.0220	0.0224	0.0214	0.0207
	0.0161	0.0217	0.0222	0.0224	0.0216	0.0211
	0.0178	0.0219	0.0223	0.0228	0.0217	0.0214
	0.0185	0.0220	0.0224	0.0227	0.0219	0.0218
	0.0202	0.0221	0.0228	0.0229	0.0222	0.0222
	0.0211	0.0226	0.0227	0.0232	0.0222	0.0222
0.050 increments	0.0215	0.0225	0.0231	0.0235	0.0227	0.0227
	0.0221	0.0229	0.0231	0.0237	0.0227	0.0227
	0.0222	0.0230	0.0234	0.0235	0.0229	0.0233
	0.0226	0.0230	0.0237	0.0238	0.0229	0.0232
	0.0228	0.0233	0.0236	0.0236	0.0232	0.0232
	0.0228	0.0234	0.0237	0.0239	0.0233	0.0232
	0.0227	0.0233	0.0233	0.0238	0.0233	0.0227
	0.0222	0.0232	0.0234	0.0237	0.0233	0.0229
	0.0222	0.0233	0.0232	0.0237	0.0229	0.0222
	0.0216	0.0231	0.0231	0.0232	0.0227	0.0221
	0.0208	0.0228	0.0227	0.0231	0.0222	0.0213
	0.0196	0.0226	0.0225	0.0227	0.0222	0.0210
	0.0176					0.0210
	0.0170					
	0.0163					
	0.0145					
↓	0.0145					

(a) Direction of travel was clockwise for all samples. See Figures 34 through 39 for reference points; 0 reference point was picked up at random and a scribe line was made along the length of the rod section before mets were cut.

(b) Z-location requested (inches from bottom of rod). Mets were numbered chronologically, as they were made and measured, rather than with respect to position along the rod.

TABLE 16. Fuel Particle Size Distribution

Rod Section	Total Weight of Fuel, g	% of Total Sample Weight Retained on Each Sieve Size: No. 3-1/2 (5.6 mm or 0.233 in.)	No. 5 (4.00 mm or 0.157 in.)	No. 7 (2.80 mm or 0.111 in.)	No. 10 (2.00 mm or 0.0787 in.)	No. 18 (1.00 mm or 0.0394 in.)	No. 50 (300 µm or 0.0117 in.)	Receiver (<300 µm or <0.0117 in.)
2D5 (1)[a]	243.753	15.98	69.84	12.69	0.71	0.23	0.25	0.31
3B5 (1)	225.212	19.88	65.57	13.35	0.71	0.08	0.19	0.22
3D5 (2)	253.991	18.66	61.03	15.83	2.20	1.13	0.73	0.42
3E5 (3)	254.497	15.20	68.18	13.80	1.49	0.53	0.38	0.41
4B5 (3)	250.466	18.88	58.28	20.28	1.53	0.44	0.27	0.31
5C5 (3)	270.867	28.49	54.95	14.92	0.74	0.38	0.24	0.30
5D5 (3)	246.704	20.13	64.58	13.61	0.64	0.31	0.32	0.42
3B5A (3)	136.598	8.43	70.17	18.97	1.22	0.37	0.33	0.52
3B5B (11)	146.223	49.83	45.00	4.52	0	0.07	0.26	0.33

(a) Number in parentheses indicates the number of whole pellets before size analysis.

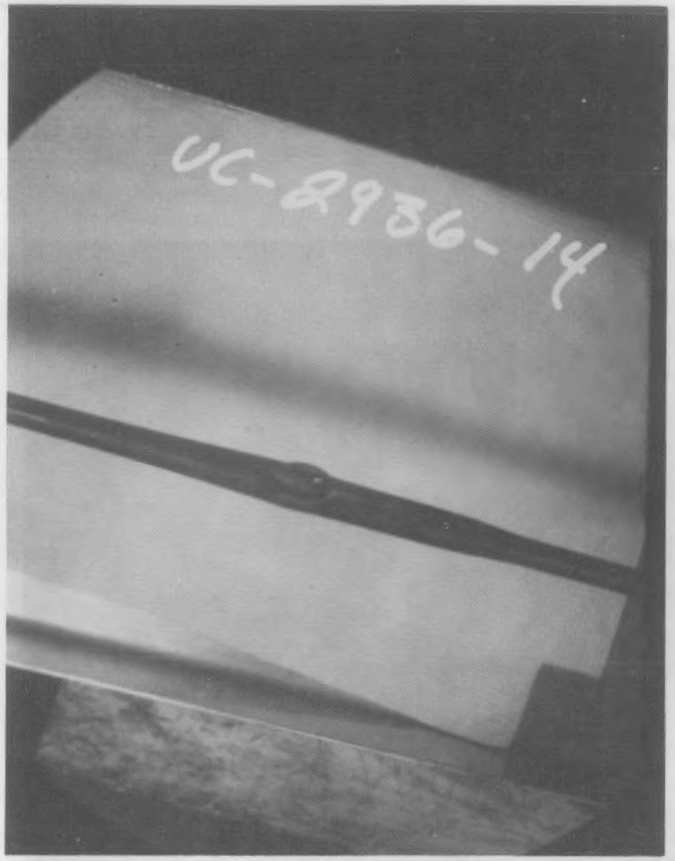

FIGURE 40. Rupture Zone of Rod Section 3B5

FIGURE 41. Fuel Fragments from Rod Section 3B5A Before Sieve Shaking

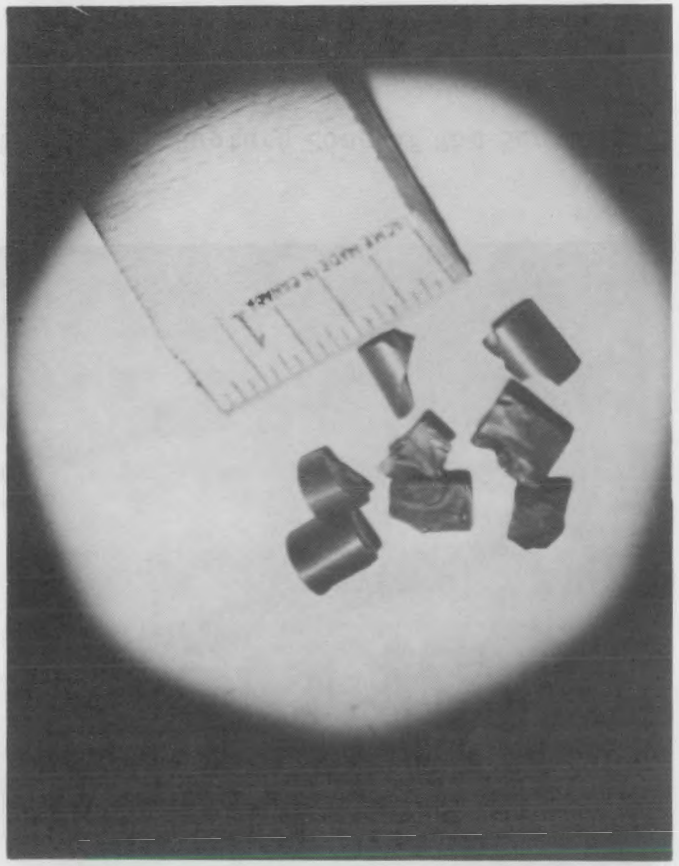

FIGURE 42. Rod Section 3B5A Fuel Fragments from Screen 1 (0.233 in., 5.6 mm)

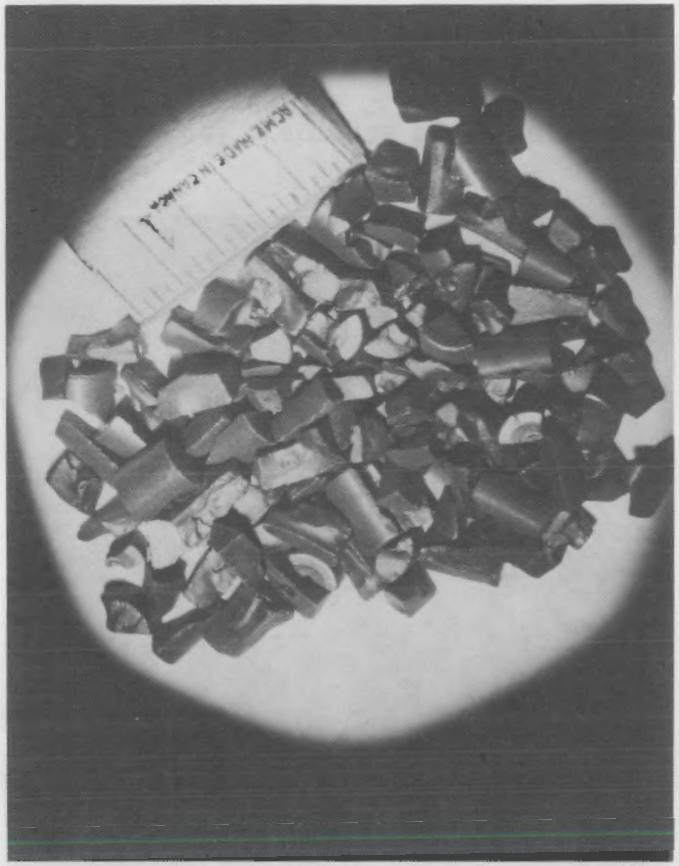

FIGURE 43. Rod Section 3B5A Fuel Fragments from Screen 2 (0.157 in., 4.0 mm)

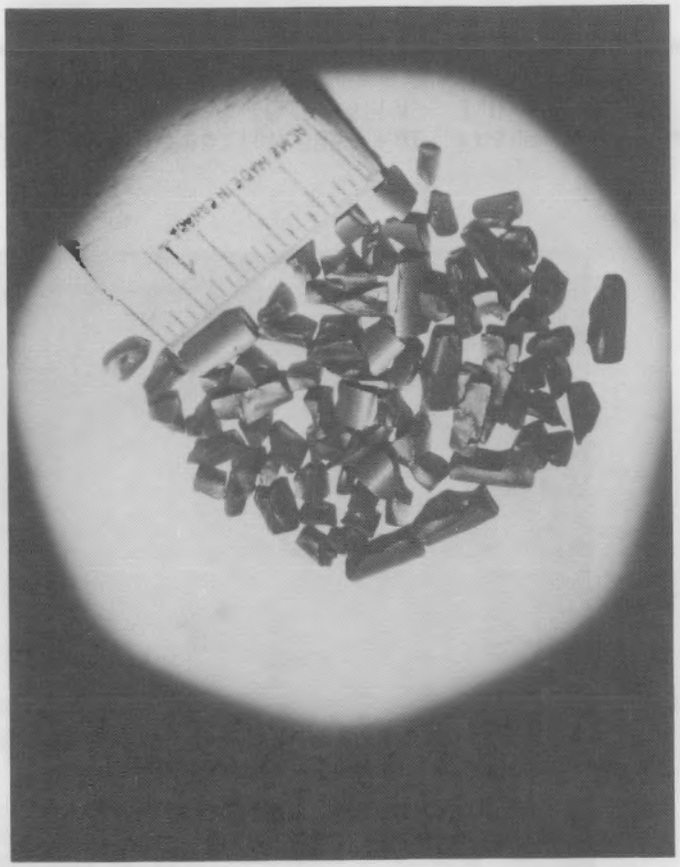

FIGURE 44. Rod Section 3B5A Fuel Fragments from Screen 3 (0.111 in., 2.8 mm)

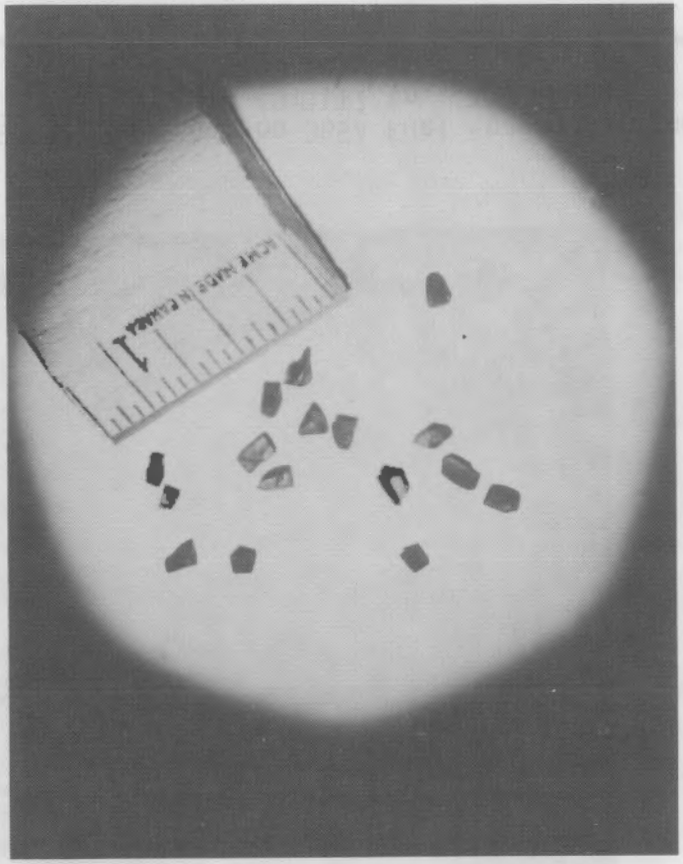

FIGURE 45. Rod Section 3B5A Fuel Fragments from Screen 4 (0.0787 in., 2.0 mm)

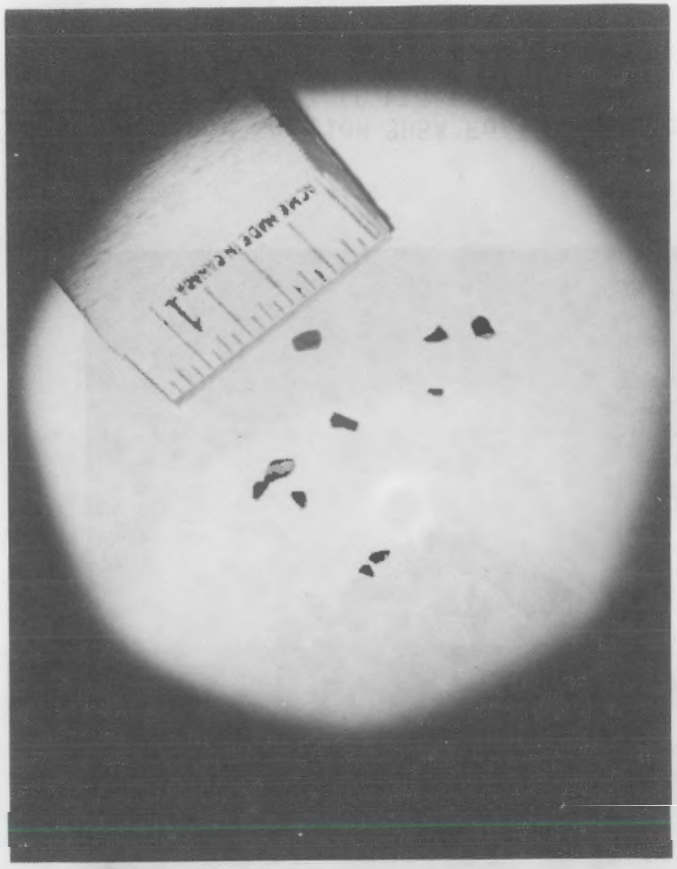

FIGURE 46. Rod Section 3B5A Fuel Fragments from Screen 5 (0.0394 in., 1.0 mm)

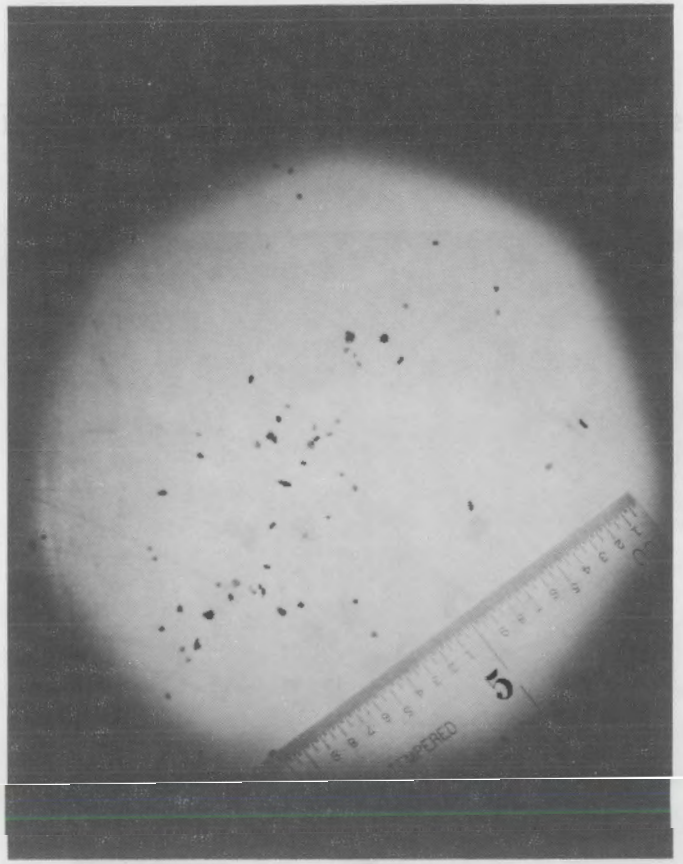

FIGURE 47. Rod Section 3B5A Fuel Fragments from Screen 6 (0.0117 in., 300 μm)

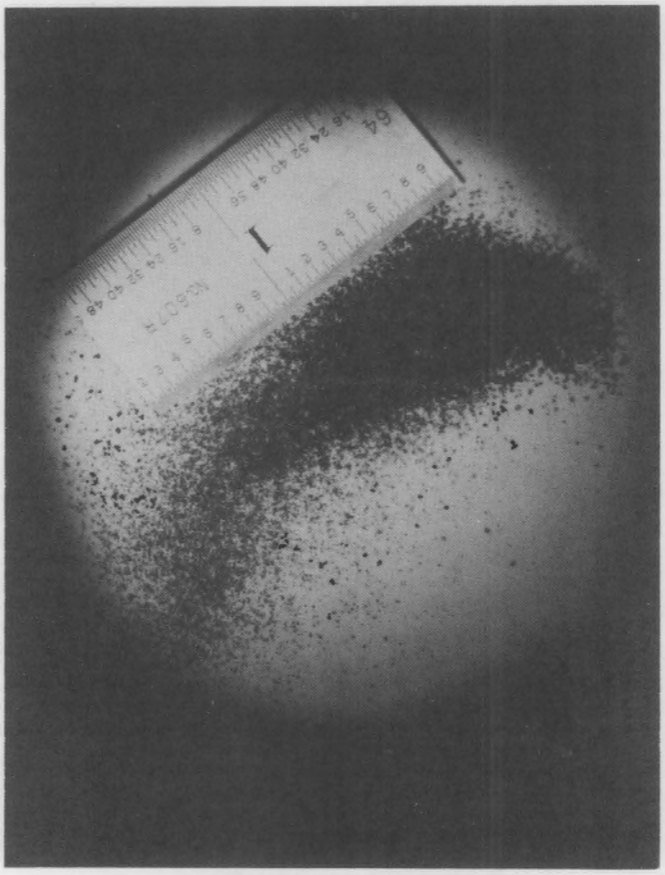

FIGURE 48. Rod Section 3B5A Fuel Fragments from Receiver (<0.0117 in., <300 μm)

REFERENCES

Guenther, R. J. 1983. Results of Simulated Abnormal Heating Events for Full-Length Nuclear Fuel Rods. PNL-4555, Pacific Northwest Laboratory, Richland, Washington.

Hann, C. R. 1979. Program Plan for LOCA Simulation in the National Research Universal (NRU) Reactor. PNL-3056, Pacific Northwest Laboratory, Richland, Washington.

Mohr, C. L., et al. 1983. LOCA Simulation in the National Research Universal Reactor Program, Data Report for the Third Materials Experiment (MT-3). NUREG/CR-2528, PNL-4166, Pacific Northwest Laboratory, Richland, Washington.

NUREG/CR-3350
PNL-4933
R3

DISTRIBUTION

No. of Copies

OFFSITE

U.S. Nuclear Regulatory Commission
Division of Technical Information and Document Control
7920 Norfolk Avenue
Bethesda, MD 20014

O. E. Bassett
U.S. Nuclear Regulatory Commission
M/S P-1102
Washington, DC 20555

P. Boehnert
U.S. Nuclear Regulatory Commission
Advisory Committee on Reactor Safeguards
M/S H-1016
Washington, DC 20555

W. Hodges
U.S. Nuclear Regulatory Commission
M/S P-1132
Washington, DC 20555

A. Hon
U.S. Nuclear Regulatory Commission
M/S 1130-SS
Washington, DC 20555

No. of Copies

W. Johnston
U.S. Nuclear Regulatory Commission
M/S P-302
Washington, DC 20555

W. Kerr
U.S. Nuclear Regulatory Commission
Advisory Committee on Reactor Safeguards
M/S H-1016
Washington, DC 20555

N. Lauben
U.S. Nuclear Regulatory Commission
M/S P-1132
Washington, DC 20555

G. Marino
U.S. Nuclear Regulatory Commission
M/S 1130-SS
Washington, DC 20555

R. Meyer
U.S. Nuclear Regulatory Commission
M/S P-1130-55
Washington, DC 20555

J. Norberg
U.S. Nuclear Regulatory Commission
M/S NL 5650
Washington, DC 20555

No. of Copies

L. Phillips
U.S. Nuclear Regulatory Commission
M/S P-924
Washington, DC 20555

D. F. Ross
U.S. Nuclear Regulatory Commission
M/S 1130-SS
Washington, DC 20555

L. S. Rubenstein
U.S. Nuclear Regulatory Commission
M/S P-932
Washington, DC 20555

P. Shewmon
U.S. Nuclear Regulatory Commission
Advisory Committee on Reactor Safeguards
M/S H-1016
Washington, DC 20555

L. Shotkin
U.S. Nuclear Regulatory Commission
M/S 1130-SS
Washington, DC 20555

20 R. Van Houten
U.S. Nuclear Regulatory Commission
M/S 1130-SS
Washington, DC 20555

J. Voglewede
U.S. Nuclear Regulatory Commission
M/S P-924
Washington, DC 20555

No. of Copies

N. Zuber
U.S. Nuclear Regulatory Commission
M/S 1130-SS
Washington, DC 20555

B. Bingham
Babcock and Wilcox Co.
P.O. Box 1200
Lynchburg, VA 24505

C. Morgan
Babcock and Wilcox Co.
P.O. Box 1200
Lynchburg, VA 24505

2 R. Duncan
Combustion Engineering
1000 Prospect Hill Road
P.O. Box 500
Windsor, CT 06095

S. Ritterbush
Combustion Engineering
1000 Prospect Hill Road
P.O. Box 500
Windsor, CT 06095

L. P. Leach
EG&G Idaho, Inc.
P.O. Box 1625
Idaho Falls, ID 83401

P. E. McDonald
EG&G Idaho, Inc.
P.O. Box 1625
Idaho Falls, ID 83401

D. Ogden
EG&G Idaho, Inc.
P.O. Box 1625
Idaho Falls, ID 83401

P. Davis (ITI)
Electric Power Research Institute
3412 Hillview Avenue
Palo Alto, CA 94022

No. of Copies

R. Duffey
Electric Power Research Institute
3412 Hillview Avenue
Palo Alto, CA 94022

M. Merilo
Electric Power Research Institute
3412 Hillview Avenue
Palo Alto, CA 94022

R. Oehlberg
Electric Power Research Institute
3412 Hillview Avenue
Palo Alto, CA 94022

W. Sun
Electric Power Research Institute
3412 Hillview Avenue
Palo Alto, CA 94022

2 G. Thomas
Electric Power Research Institute
3412 Hillview Avenue
Palo Alto, CA 94022

L. Thompson
Electric Power Research Institute
3412 Hillview Avenue
Palo Alto, CA 94022

S. Armijo
General Electric Company
175 Curtner Avenue
San Jose, CA 95114

L. Noble
General Electric Company
175 Curtner Avenue
San Jose, CA 95114

No. of Copies

N. Shirley
General Electric Company
175 Curtner Avenue
San Jose, CA 95114

G. Sozzi
General Electric Company
175 Curtner Avenue
San Jose, CA 95114

R. Williams
General Electric Company
175 Curtner Avenue
San Jose, CA 95114

W. Kirchner
Los Alamos Scientific Laboratory
P.O. Box 1663
Los Alamos, NM 87544

D. M. Chapin
MPR Associates, Inc.
1140 Connecticut Avenue, NW
Washington, DC 20036

J. Davis
Nuclear Engineering Department
Potomac Electric Avenue, NW
Washington, DC 20068

2 R. Chapman
Oak Ridge National Laboratory
P.O. Box X
Oak Ridge, TN 37830

F. Mynatt
Oak Ridge National Laboratory
P.O. Box X
Oak Ridge, TN 37830

2 D. Burman
Westinghouse Electric Corporation
P.O. Box 355
Pittsburgh, PA 15230

No. of Copies

2 L. D. Hochreiter
Westinghouse Electric Corporation
P.O. Box 355
Pittsburgh, PA 15230

R. Rosal
Westinghouse Electric Corporation
P.O. Box 355
Pittsburgh, PA 15230

FOREIGN

M. D. Atfield
Chalk River Nuclear Laboratories
Atomic Energy of Canada, Ltd.
Chalk River, Ontario, Canada
K0J 1J0

D. J. Axford
Chalk River Nuclear Laboratories
Atomic Energy of Canada, Ltd.
Chalk River, Ontario, Canada
K0J 1J0

D. Hall
Chalk River Nuclear Laboratories
Atomic Energy of Canada, Ltd.
Chalk River, Ontario, Canada
K0J 1J0

C. A. Herriot
Chalk River Nuclear Laboratories
Atomic Energy of Canada, Ltd.
Chalk River, Ontario, Canada
K0J 1J0

J. W. Logie
Chalk River Nuclear Laboratories
Atomic Energy of Canada, Ltd.
Chalk River, Ontario, Canada
K0J 1J0

No. of Copies

I. C. Martin
Chalk River Nuclear Laboratories
Atomic Energy of Canada, Ltd.
Chalk River, Ontario, Canada
K0J 1J0

6 D. T. Nishimura
Chalk River Nuclear Laboratories
Atomic Energy of Canada, Ltd.
Chalk River, Ontario, Canada
K0J 1J0

M.J.F. Notley
Chalk River Nuclear Laboratories
Atomic Energy of Canada, Ltd.
Chalk River, Ontario, Canada
K0J 1J0

A. Okazaki
Chalk River Nuclear Laboratories
Atomic Energy of Canada, Ltd.
Chalk River, Ontario, Canada
K0J 1J0

D. Thompson
Chalk River Nuclear Laboratories
Atomic Energy of Canada, Ltd.
Chalk River, Ontario, Canada
K0J 1J0

A. Smith
Chalk River Nuclear Laboratories
Atomic Energy of Canada, Ltd.
Chalk River, Ontario, Canada
K0J 1J0

4 T. Healey
Central Electricity Generating Board
Berkeley Nuclear Laboratories
Berkeley, Gloucestershire GL13 9PB
England

No. of Copies

4 M. Ishikawa, Chief
Reactivity Accident Laboratory
Japan Atomic Energy Research Institute
Tokai Research Establishment
Tokai-Mura, Naka-Gun
Ibaraki-Ken
Japan

S. Kawasaki
Fuel Reliability Lab III
Division of Reactor Safety
Japan Atomic Energy Research Institute
Tokai Research Establishment
Tokai-Mura, Naka-Gun
Ibaraki-Ken
Japan

T. Doyle
JRC-ISPRA, EURATOM
CCR ESSOR Division
21020 Cento Euratom Di Ispra (Varese)
Italy

H. Holtbecker
JRC-ISPRA, EURATOM
CCR ESSOR Division
21020 Cento Euratom Di Ispra (Varese)
Italy

J. Randles
JRC-ISPRA, EURATOM
CCR ESSOR Division
21020 Cento Euratom Di Ispra (Varese)
Italy

O. Simoni
JRC-ISPRA, EURATOM
CCR ESSOR Division
21020 Cento Euratom Di Ispra (Varese)
Italy

No. of Copies

F. Erbacher
Kernforschungzentrum Karlsruhe
Weberstrasse 5
75 Karlsruhe 1
Federal Republic of Germany

A. Fiege
Kernforschungzentrum Karlsruhe
Weberstrasse 5
75 Karlsruhe 1
Federal Republic of Germany

2 H. Rininslandd
Kernforschungzentrum Karlsruhe
Weberstrasse 5
75 Karlsruhe 1
Federal Republic of Germany

2 J. H. Gittus
United Kingdom Atomic Energy Authority
Atomic Energy Tech. Branch
Harwell, DIDCOT
Oxfordshire OX11 ORA
England

C. A. Mann
Springfields Nuclear Power Development Laboratory
United Kingdom Atomic Energy Authority
Springfields, Salwick
Preston PR 4 ORR
England

3 I. H. Gibson
Atomic Energy Establishment Winfrith
Dorchester, Dorset DT2-8DH
England

No. of Copies

ONSITE

4 Exxon Nuclear Company, Inc.

T. Doyle
W. Kayser
J. Morgan
W. Nechodom

50 Pacific Northwest Laboratory

W. J. Bailey
J. O. Barner
M. D. Freshley
R. L. Goodman
R. J. Guenther
C. R. Hann
G. M. Hesson
U. P. Jenquin
L. L. King
R. R. Lewis (2)
E. E. Panisko
L. J. Parchen
J. P. Pilger
W. N. Rausch (26)
G. E. Russcher
B. J. Webb
N. J. Wildung
Publishing Coordination (2)
Technical Information (5)

NRC FORM 335 (11-81) U.S. NUCLEAR REGULATORY COMMISSION

BIBLIOGRAPHIC DATA SHEET

1. REPORT NUMBER (Assigned by DDC)
NUREG/CR-3350
PNL-4933

4. TITLE AND SUBTITLE (Add Volume No., if appropriate)
LOCA Simulation in the National Research Universal Reactor Program: Postirradiation Examination Results for the Third Materials Experiment (MT-3)

2. (Leave blank)

3. RECIPIENT'S ACCESSION NO.

7. AUTHOR(S)
W. N. Rausch

5. DATE REPORT COMPLETED
MONTH December YEAR 1983

9. PERFORMING ORGANIZATION NAME AND MAILING ADDRESS (Include Zip Code)
Pacific Northwest Laboratory
Box 999
Richland, WA 99352

DATE REPORT ISSUED
MONTH April YEAR 1984

6. (Leave blank)

8. (Leave blank)

12. SPONSORING ORGANIZATION NAME AND MAILING ADDRESS (Include Zip Code)
Division of Accident Evaluation
Office of Nuclear Regulatory Research
U. S. Nuclear Regulatory Commission
Washington, D. C. 20555

10. PROJECT/TASK/WORK UNIT NO.

11. FIN NO.
B2277

13. TYPE OF REPORT
Topical

PERIOD COVERED (Inclusive dates)

15. SUPPLEMENTARY NOTES

14. (Leave blank)

16. ABSTRACT (200 words or less)

A series of in-reactor experiments were conducted by Pacific Northwest Laboratory, using full-length 32-rod pressurized water reactor fuel bundles,as part of the Loss-of-Coolant Accident (LOCA) Simulation Program. The third materials experiment (MT-3) was the sixth in the series of thermal-hydraulic and materials deformation/rupture experiments conducted in the National Research Universal (NRU) reactor, Chalk River, Ontario, Canada. MT-3 was jointly funded by the U.S. Nuclear Regulatory Commission and the United Kingdom Atomic Energy Authority. The experiment evaluated ballooning and rupture during active two-phase cooling in the temperature range from 1400 to 1500 F. The 12 test rods in the center of the 32-rod bundle were initially pressurized to 550 psi to insure rupture in the correct temperature range. All 12 of the rods ruptured, with an average peak bundle strain of about 55%. A hot cell postirradiation examination (PIE) of several of the ruptured rods was also conducted. This report describes the work performed and presents the PIE results. Information obtained during the PIE analysis included cladding thickness measurements, metallography, and particle size analysis of the cracked and broken fuel pellets.

17. KEY WORDS AND DOCUMENT ANALYSIS
postirradiation examination (PIE)
cladding deformation/rupture
alpha grain growth
textural banding

17a. DESCRIPTORS
Loss-of-coolant accident (LOCA)
Materials Test 3 (MT-3)

17b. IDENTIFIERS/OPEN-ENDED TERMS

18. AVAILABILITY STATEMENT
Unlimited

19. SECURITY CLASS (This report)
Unclassified

21. NO. OF PAGES

20. SECURITY CLASS (This page)
Unclassified

22. PRICE
$

NRC FORM 335 (11-81)